INSTITUTE for NUCLEAR THEORY

BNL-INT Joint Workshop: Bridging Theory and Experiment at the Electron-Ion Collider

June 2, 2025 - June 6, 2025

ORGANIZERS

Alessandro Bacchetta
Università di Pavia
alessandro.bacchetta@unipv.it

Wim Cosyn
Florida International University
wcosyn@fiu.edu

Felix Ringer
Stony Brook University
felix.ringer@stonybrook.edu

Anna Stasto
Penn State University
ams52@psu.edu

PROGRAM COORDINATOR

Paris Nguyen
Institute for Nuclear Theory
paris90@uw.edu

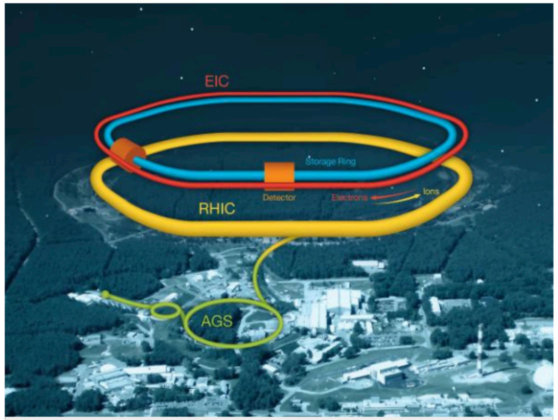

Image: Courtesy of Brookhaven National Lab

The application deadline for this event has passed.

Recent updates on (polarized) TMD extractions

INFN Istituto Nazionale di Fisica Nucleare
Sezione Pavia

Marco Radici

Processes with factorization

SIDIS

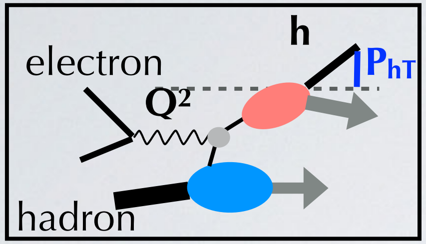

factorization conditions

$$M^2 \ll Q^2 \qquad q_T^2 = \frac{P_{hT}^2}{z^2} \ll Q^2$$

Fourier Transf. to b_T space:
from convolution to simple product

$$\frac{d\sigma}{dx\,dz\,dq_T\,dQ} \sim \mathscr{H}^{\mathrm{SIDIS}}(Q^2)\,\frac{1}{2\pi}\int_0^\infty db_T\, b_T\, J_0(b_T, q_T)\;\tilde{f}_1^{q}(x, b_T^2; Q^2)\;\tilde{D}_1^{q\to h}(z, b_T^2; Q^2)$$

hard part — TMDPDF — TMDFF

Ji, Ma, Yuan, P.R. D**71** (05); Rogers & Aybat, P.R. D**83** (11)
Collins & Metz, P.R.L. **93** (04) 252001

Drell-Yan

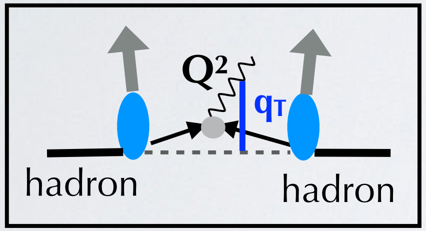

$$M^2 \ll Q^2 \qquad q_T^2 \ll Q^2$$

$$\frac{d\sigma}{dq_T\,dy\,dQ} \sim \mathscr{H}^{\mathrm{DY}}(Q^2)\,\frac{1}{2\pi}\int_0^\infty db_T\, b_T\, J_0(b_T, q_T)\;\tilde{f}_1^{\bar{q}}(x_A, b_T^2; Q^2)\;\tilde{f}_1^{q}(x_B, b_T^2; Q^2)$$

hard part — TMDPDF — TMDPDF

Collins, Soper, Sterman, N.P. B**250** (85) 199
Echevarria, Idilbi, Scimemi, JHEP **07** (12)

e+ e-

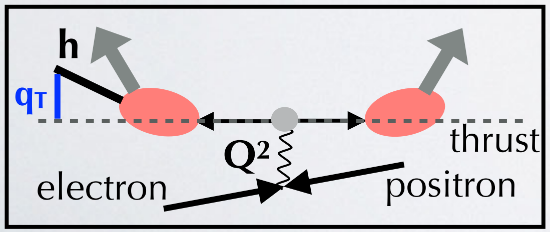

$$M_h^2 \ll Q^2 \qquad q_T^2 = \frac{P_{hT}^2}{z^2} \ll Q^2$$

Factorized expression for
but data only for spin asymmetries

$$\frac{d\sigma}{dz_1\,dz_2\,dq_T\,d\Omega} \sim \text{TMDFF} \otimes \text{TMDFF}$$

Collins & Soper, N.P. B**193** (81) 381

For e+ e- → h+X formula more complicated; need to include info on thrust axis

Boglione & Simonelli, JHEP **02** (21) 076; **02** (22) 013; **09** (23) 006

Processes with factorization

SIDIS

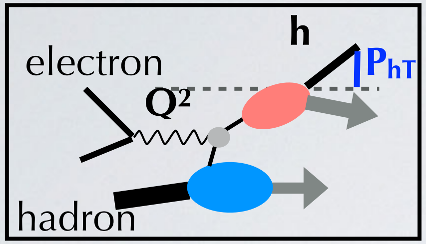

factorization conditions

$$M^2 \ll Q^2 \qquad q_T^2 = \frac{P_{hT}^2}{z^2} \ll Q^2$$

Fourier Transf. to b_T space: from convolution to simple product

$$\frac{d\sigma}{dx\,dz\,dq_T\,dQ} \sim \mathscr{H}^{\rm SIDIS}(Q^2)\,\frac{1}{2\pi}\int_0^\infty db_T\, b_T\, J_0(b_T, q_T)\;\tilde{f}_1^q(x, b_T^2; Q^2)\;\tilde{D}_1^{q\to h}(z, b_T^2; Q^2)$$

hard part — TMDPDF — TMDFF

Ji, Ma, Yuan, P.R. D**71** (05); Rogers & Aybat, P.R. D**83** (11)
Collins & Metz, P.R.L. **93** (04) 252001

Drell-Yan

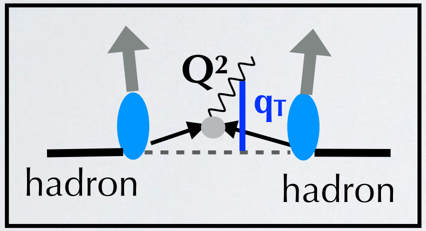

$$M^2 \ll Q^2 \qquad q_T^2 \ll Q^2$$

$$\frac{d\sigma}{dq_T\,dy\,dQ} \sim \mathscr{H}^{\rm DY}(Q^2)\,\frac{1}{2\pi}\int_0^\infty db_T\, b_T\, J_0(b_T, q_T)\;\tilde{f}_1^{\bar{q}}(x_A, b_T^2; Q^2)\;\tilde{f}_1^q(x_B, b_T^2; Q^2)$$

hard part — TMDPDF — TMDPDF

Collins, Soper, Sterman, N.P. B**250** (85) 199
Echevarria, Idilbi, Scimemi, JHEP **07** (12)

e+ e-

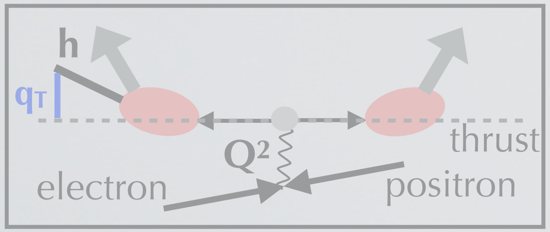

$$M_h^2 \ll Q^2 \qquad q_T^2 = \frac{P_{hT}^2}{z^2} \ll Q^2$$

Factorized expression for

$$\frac{d\sigma}{dz_1\,dz_2\,dq_T\,d\Omega} \sim \text{TMDFF} \otimes \text{TMDFF}$$

but data only for spin asymmetries

Collins & Soper, N.P. B**193** (81) 381

For e+ e- → h+X formula more complicated; need to include info on thrust axis

Boglione & Simonelli, JHEP **02** (21) 076; **02** (22) 013; **09** (23) 006

Phase space for processes with factorization

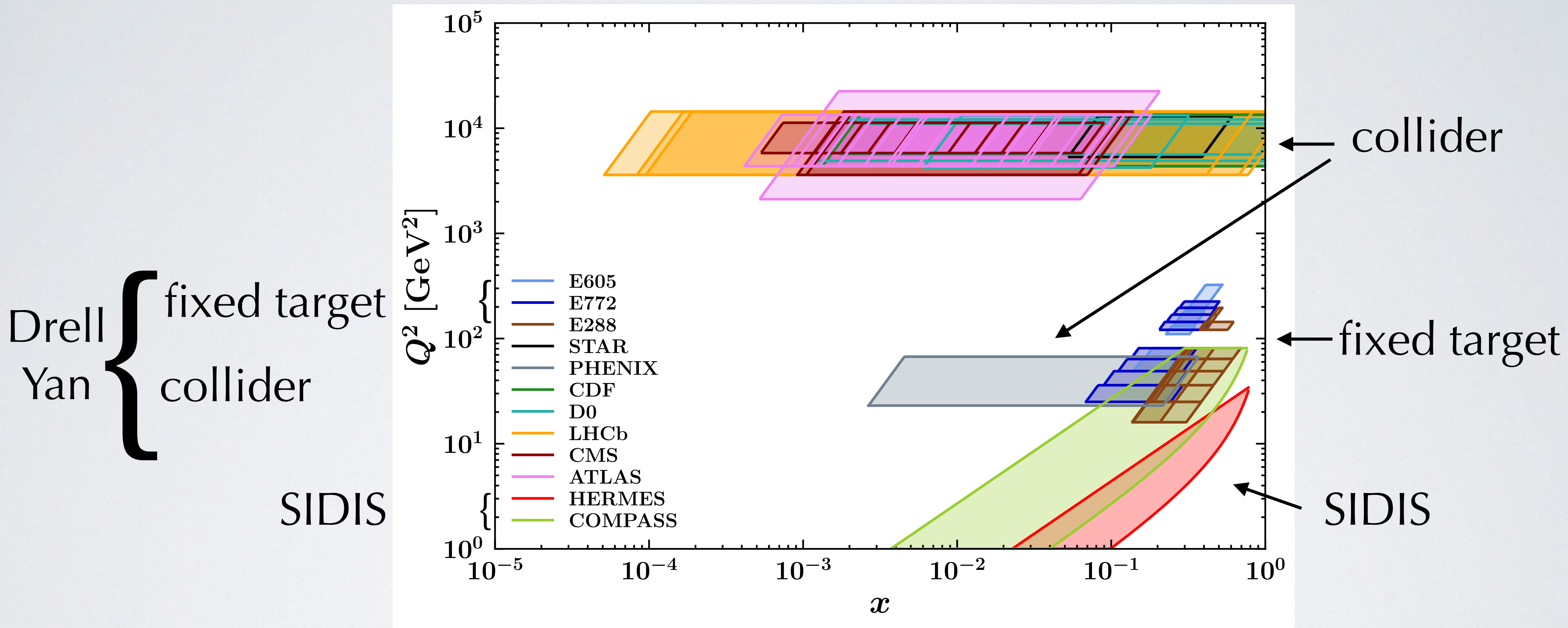

Evolution of TMDs

Collins - Soper - Sterman (CSS) scheme

Collins, "Foundations of Perturbative QCD" (11)

$$\tilde{f}_1^q(x, b_T^2; \mu_f, \zeta_f) = \quad \text{Evo}\left[(\mu_f, \zeta_f) \leftarrow (\mu_i, \zeta_i)\right] \times \tilde{f}_1^q(x, b_T^2; \mu_i, \zeta_i)$$

small b_T → OPE

large b_T ?

$$\sum_i \left[C_{qi}(x, b_T; \mu_i, \zeta_i) \otimes f_1^i(x, \mu_i)\right]$$

PDF

Evolution operator,
Wilson Coefficient C,
are all perturbatively
calculable

$\overline{\text{MS}}$ choice (cancel large logs in resummation)

$$\mu_i = \sqrt{\zeta_i} = 2e^{-\gamma_E} / b_T$$

Evolution of TMDs

Collins - Soper - Sterman (CSS) scheme

Collins, "Foundations of Perturbative QCD" (11)

$$\tilde{f}_1^q(x, b_T^2; \mu_f, \zeta_f) = \text{Evo}\left[(\mu_f, \zeta_f) \leftarrow (\mu_i, \zeta_i)\right] \times \tilde{f}_1^q(x, b_T^2; \mu_i, \zeta_i) \times \tilde{f}_{NP}(x, b_T^2; Q_0^2)$$

small b_T → OPE:

$$\sum_i \left[C_{qi}(x, b_T; \mu_i, \zeta_i) \otimes f_1^i(x, \mu_i) \right]$$

PDF

large b_T →

$$\lim_{b_T \to 0} \tilde{f}_{NP} = 1$$

parametrized at Q_0 and fitted to data

Evolution operator, Wilson Coefficient C, are all perturbatively calculable

$\overline{\text{MS}}$ choice (cancel large logs in resummation)

$$\mu_i = \sqrt{\zeta_i} = 2e^{-\gamma_E} / b_T$$

smooth connection with large b_T
replace b_T with $b^*(b_T)$

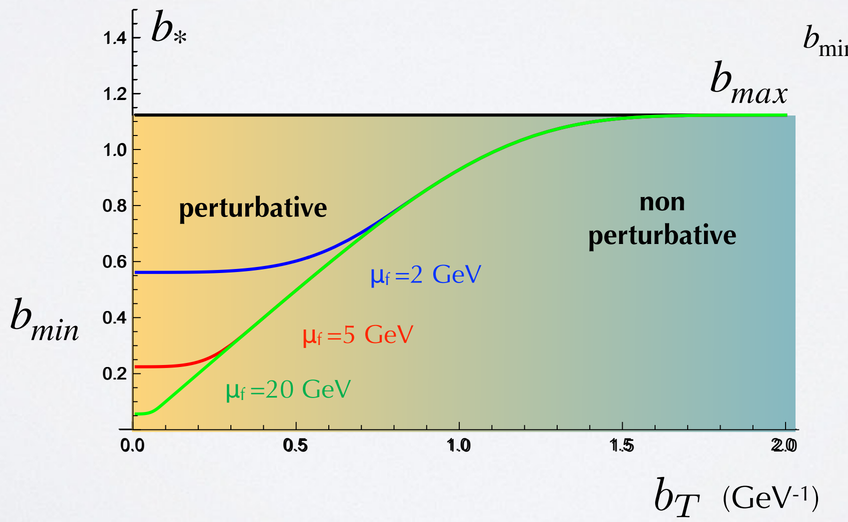

$$b_{\min} = \frac{2e^{-\gamma_E}}{\mu_f} \longleftarrow b_*(b_T) \longrightarrow b_{\max} = \frac{2e^{-\gamma_E}}{Q_0}$$

$$\mu_f \geq \mu_{b_*} = \frac{2e^{-\gamma_E}}{b_*(b_T)} \geq 1$$

b_{min} prescription facilitates matching to fixed-order

Bozzi et al., P.L. **B696** (11) 207

not used in all extractions

Evolution of TMDs

Collins - Soper - Sterman (CSS) scheme

Collins, "Foundations of Perturbative QCD" (11)

$$\tilde{f}_1^q(x, b_T^2; \mu_f, \zeta_f) = \text{Evo}\left[(\mu_f, \zeta_f) \leftarrow (\mu_i, \zeta_i)\right] \times \tilde{f}_1^q(x, b_T^2; \mu_i, \zeta_i) \times \tilde{f}_{NP}(x, b_T^2; Q_0^2)$$

small b_T → OPE, PDF:

$$\sum_i \left[C_{qi}(x, b_T; \mu_i, \zeta_i) \otimes f_1^i(x, \mu_i)\right]$$

large b_T → $\tilde{f}_{NP}$:

$$\lim_{b_T \to 0} \tilde{f}_{NP} = 1$$

parametrized at Q_0 and fitted to data

Final formula

evolution in μ — evolution in ζ

$$\tilde{f}_1^q(x, b_T^2; \mu_f, \zeta_f) = \exp\left[\int_{\mu_{b_*}}^{\mu_f} \frac{d\mu}{\mu}\left(\gamma_F - \gamma_K \log\frac{\sqrt{\zeta_f}}{\mu}\right)\right] \exp\left[K(b_*, \mu_b) \log\frac{\sqrt{\zeta_f}}{\mu_b}\right]$$

$$\times \sum_i \left[C_{qi}(x, b_*; \mu_b, \mu_b^2) \otimes f_1^i(x, \mu_b)\right]$$

$$\times \exp\left[g_K(b_T) \log\frac{\sqrt{\zeta_f}}{Q_0}\right] f_{\text{NP}}(x, b_T)$$

similar formula for $\tilde{D}_1^{q \to h}$

Quality of TMD extraction:

- perturbative accuracy
- size of data set and best χ^2

Logarithmic counting

$$\frac{d\sigma}{dx\,dz\,dq_T\,dQ} \sim \mathcal{H}^{\text{SIDIS}}(Q^2)\,\frac{1}{2\pi}\int_0^\infty db_T\, b_T\, J_0(b_T, q_T)\;\tilde{f}_1^q(x, b_T^2; Q, Q^2)\;\tilde{D}_1^{q\to h}(z, b_T^2; Q, Q^2)$$

$$\tilde{f}_1^q(x, b_T^2; \mu_f, \zeta_f) = \exp\left[\int_{\mu_{b_*}}^{\mu_f}\frac{d\mu}{\mu}\left(\gamma_F - \gamma_K\,\log\frac{\sqrt{\zeta_f}}{\mu}\right)\right]\exp\left[K(b_*, \mu_b)\,\log\frac{\sqrt{\zeta_f}}{\mu_b}\right]\;\times\exp\left[g_K(b_T)\log\frac{\sqrt{\zeta_f}}{Q_0}\right] f_{\text{NP}}(x, b_T)$$

$$\times\sum_i\left[C_{qi}(x, b_*; \mu_b, \mu_b^2)\otimes f_1^i(x, \mu_b)\right]$$

similar formula for $\tilde{D}_1^{q\to h}$

perturbative

α_S^n

accuracy	$\mathcal{H}$ and C	K and γ_F	γ_K	PDF and α_S	FF
LL	0	-	1	-	-
NLL	0	1	2	LO	LO
NLL’	1	1	2	NLO	NLO
NNLL	1	2	3	NLO	NLO
NNLL’	2	2	3	NNLO	NNLO
N^3LL(-)	2	3	4	NNLO	NLO
N^3LL	2	3	4	NNLO	NNLO
N^3LL’	3	3 4	5	N^3LO	N^3LO
N^4LL(-)	3	3 4	5	N^3LO	NNLO
N^4LL	3	3 4	5	N^3LO	N^3LO

The unpolarized quark TMD PDF

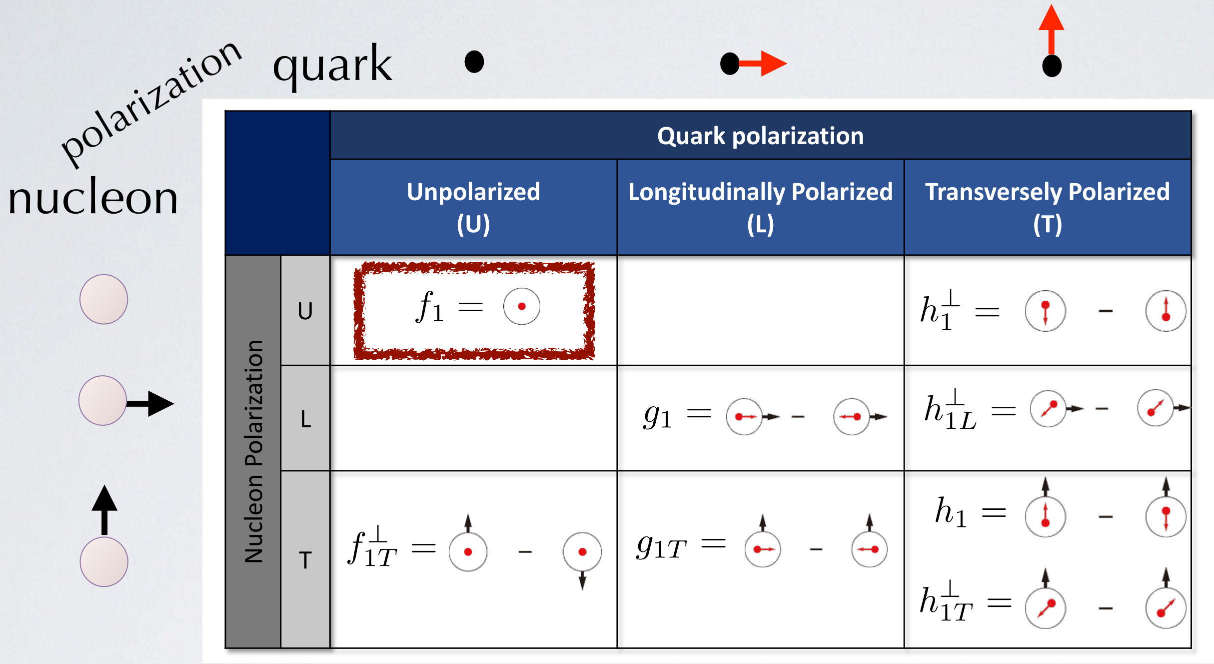

Mulders & Tangerman, N.P. **B461** (96)
Boer & Mulders, P.R. D**57** (98)

Let's focus on the simplest unpolarized TMD PDF:

f_1^q = probability density to find an unpolarized quark q with light-cone momentum fraction x and transverse momentum $\mathbf{k}_\perp$ in an unpolarized hadron

It enters the denominator of every spin asymmetry needed to extract the other polarized TMDs:

$$A = \frac{d\sigma(\text{pol.}) - d\sigma(-\text{pol.})}{d\sigma(\text{pol.}) + d\sigma(-\text{pol.}) \equiv d\sigma^0}$$

Most recent extractions of Nucleon TMD f_1

	Accuracy	SIDIS	Drell-Yan	N of points	χ^2/N_{points}	Flavor dep.
PV 2017 arXiv:1703.10157	NLL	✔	✔	8059	1.5	✘
SV 2017 arXiv:1706.01473	N^3LL	✘	✔ (LHC)	309	1.23	✘
BSV 2019 arXiv:1902.08474	N^3LL	✘	✔ (LHC)	457	1.17	✘
SV 2019 arXiv:1912.06532	N^3LL(-)	✔	✔ (LHC)	1039	1.06	✘
PV 2019 arXiv:1912.07550	N^3LL	✘	✔ (LHC)	353	1.07	✘
MAPTMD 2022 arXiv:2206.07598	N^3LL(-)	✔	✔ (LHC)	2031	1.06	✘
ART23 arXiv:2305.07473	N^4LL(-)	✘	✔ (LHC)	627	0.96	✔
MAPTMD 2024 arXiv:2405.13833	N^3LL	✔	✔ (LHC)	2031	1.08	✔
MAPNN 2025 arXiv:2502.04166	N^3LL	✘	✔ (LHC)	482	0.97	✘
ART25 arXiv:2503.11201	N^4LL(-)	✔	✔ (LHC)	1209	1.05	✔

Most recent extractions of Nucleon TMD f_1

	Accuracy	SIDIS	Drell-Yan	N of points	χ^2/N_{points}	Flavor dep.
PV 2017 arXiv:1703.10157	NLL	✔	✔	8059	1.5	✘
SV 2017 arXiv:1706.01473	N^{3}LL	✘	✔ (LHC)	309	1.23	✘
BSV 2019 arXiv:1902.08474	N^{3}LL	✘	✔ (LHC)	457	1.17	✘
SV 2019 arXiv:1912.06532	N^{3}LL(-)	✔	✔ (LHC)	1039	1.06	✘
PV 2019 arXiv:1912.07550	N^{3}LL	✘	✔ (LHC)	353	1.07	✘
MAPTMD 2022 arXiv:2206.07598	N^{3}LL(-)	✔	✔ (LHC)	2031	1.06	✘
ART23 arXiv:2305.07473	N^{4}LL(-)	✘	✔ (LHC)	627	0.96	✔
MAPTMD 2024 arXiv:2405.13833	N^{3}LL	✔	✔ (LHC)	2031	1.08	✔
MAPNN 2025 arXiv:2502.04166	N^{3}LL	✘	✔ (LHC)	482	0.97	✘
ART25 arXiv:2503.11201	N^{4}LL(-)	✔	✔ (LHC)	1209	1.05	✔

increasing accuracy & precision

Most recent extractions of Nucleon TMD f_1

	Accuracy	SIDIS	Drell-Yan	N of points	χ^2/N_{points}	Flavor dep.
PV 2017 arXiv:1703.10157	NLL	✔	✔	8059	1.5	✘
SV 2017 arXiv:1706.01473	N^3LL	✘	✔ (LHC)	309	1.23	✘
BSV 2019 arXiv:1902.08474	N^3LL	✘	✔ (LHC)	457	1.17	✘
SV 2019 arXiv:1912.06532	$N^3LL(-)$	✔	✔ (LHC)	1039	1.06	✘
PV 2019 arXiv:1912.07550	N^3LL	✘	✔ (LHC)	353	1.07	✘
MAPTMD 2022 arXiv:2206.07598	$N^3LL(-)$	✔	✔ (LHC)	2031	1.06	✘
ART23 arXiv:2305.07473	$N^4LL(-)$	✘	✔ (LHC)	627	0.96	✔
MAPTMD 2024 arXiv:2405.13833	N^3LL	✔	✔ (LHC)	2031	1.08	✔
MAPNN 2025 arXiv:2502.04166	N^3LL	✘	✔ (LHC)	482	0.97	✘
ART25 arXiv:2503.11201	$N^4LL(-)$	✔	✔ (LHC)	1209	1.05	✔

global fits

first use of Neural Networks

More pheno studies on unpolarized TMD f_1

- TMD FFs from e+e- data

Boglione & Simonelli, JHEP **02** (21) 076; **02** (22) 013; **09** (23) 006

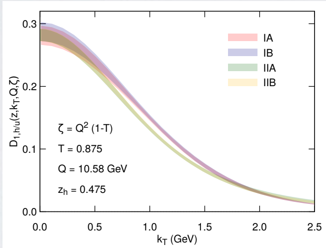

- pion TMDs

Cerutti et al. (MAP), P.R. D**107** (23) 014014
Vladimirov, JHEP **10** (19) 090
Barry et al. (JAM), P.R. D**108** (23) L091504

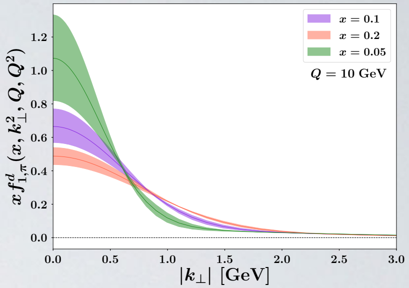

- hadron-in-jet production at colliders

D'Alesio et al., P.L. B**773** (17) 300
Kang et al., P.L. B**774** (17) 635
Arratia et al., P.R. D**102** (20) 074015

- Di-jet and heavy-meson production at colliders and in DIS

Del Castillo et al., JHEP **03** (22) 047
Gutierrez-Reyes et al., P.R.L. **121** (18) 162001

- parton-branching method

Bermudez Martinez et al., P.R. D**99** (19) 074008

- q_T-resummation based extractions

Camarda, Ferrera, Schott, E.P.J. C**84** (24) 39

- gluon TMDs

(see talks by D. Boer, A. Mukherjee and C. Pisano)

low-q_T spectrum of Higgs production in gluon fusion

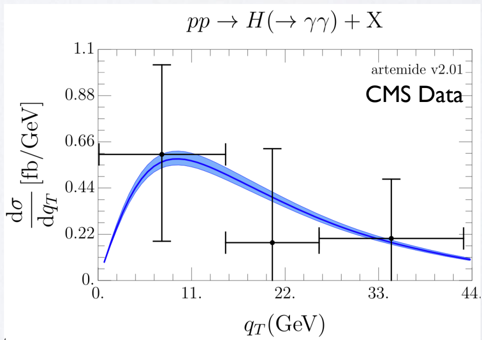

Gutierrez-Reyes et al., JHEP **11** (19) 121

Most recent extractions of Nucleon TMD f_1

	Accuracy	SIDIS	Drell-Yan	N of points	χ^2/N_{points}	Flavor dep.
PV 2017 arXiv:1703.10157	NLL	✔	✔	8059	1.5	✘
SV 2017 arXiv:1706.01473	N^3LL	✘	✔ (LHC)	309	1.23	✘
BSV 2019 arXiv:1902.08474	N^3LL	✘	✔ (LHC)	457	1.17	✘
SV 2019 arXiv:1912.06532	$N^3LL(-)$	✔	✔ (LHC)	1039	1.06	✘
PV 2019 arXiv:1912.07550	N^3LL	✘	✔ (LHC)	353	1.07	✘
MAPTMD 2022 arXiv:2206.07598	$N^3LL(-)$	✔	✔ (LHC)	2031	1.06	✘
ART23 arXiv:2305.07473	$N^4LL(-)$	✘	✔ (LHC)	627	0.96	✔
MAPTMD 2024 arXiv:2405.13833	N^3LL	✔	✔ (LHC)	2031	1.08	✔
MAPTMDNN 2025 arXiv:2502.04166	N^3LL	✘	✔ (LHC)	482	0.97	✘
ART25 arXiv:2503.11201	$N^4LL(-)$	✔	✔ (LHC)	1209	1.05	✔

MAPTMD24 settings (in one slide..)

Bacchetta et al. (MAP), JHEP **08** (24) 232

$$b_*(b_T) = b_{\max} \left(\frac{1 - e^{-b_T^4/b_{\max}^4}}{1 - e^{-b_T^4/b_{\min}^4}} \right)^{\frac{1}{4}} \qquad \begin{aligned} b_{\max} &= 2e^{-\gamma_E}/Q_0\,(=1) \\ b_{\min} &= 2e^{-\gamma_E}/Q \end{aligned}$$

same as MAPTMD22

Bacchetta et al. (MAP), JHEP **10** (22) 127

non-pert. Collins-Soper kernel $g_K(b_T) = -\, g_2^2\, b_T^2/2$

$f_{\rm NP}(x, b_T)$ Fourier Transf. of combination of 2 Gaussians + 1 weighted Gaussian, all with x-dependent widths

$D_{\rm NP}(z, b_T)$ Fourier Transf. of combination of 2 Gaussians with z-dep. widths

cuts

$\langle Q \rangle > 1.4$ GeV

$0.2 < z < 0.7$

Drell-Yan $q_T < 0.2\, Q$

SIDIS

$P_{hT} < \min\left[\min\left[0.2\, Q,\, 0.5\, Qz\right] + 0.3\,\text{GeV},\, zQ\right]$

N = 2031 pts.

MAPTMD24 settings (in one slide..)

Bacchetta et al. (MAP), JHEP **08** (24) 232

$$b_*(b_T) = b_{\max}\left(\frac{1-e^{-b_T^4/b_{\max}^4}}{1-e^{-b_T^4/b_{\min}^4}}\right)^{\frac{1}{4}} \qquad b_{\max} = 2e^{-\gamma_E}/Q_0\,(=1) \qquad b_{\min} = 2e^{-\gamma_E}/Q$$

non-pert. Collins-Soper kernel $g_K(b_T) = -\,g_2^2\, b_T^2/2$

same as MAPTMD22
Bacchetta et al. (MAP), JHEP **10** (22) 127

$f_{\rm NP}(x, b_T)$ Fourier Transf. of combination of 2 Gaussians + 1 weighted Gaussian, all with x-dependent widths for $u, d, \bar{u}, \bar{d}$, sea

$D_{\rm NP}(z, b_T)$ Fourier Transf. of combination of 2 Gaussians with z-dep. widths for fav./unfav. $u \to \pi^+ / d \to \pi^+$ and fav./unfav. $u \to K^+, \bar{s} \to K^+ / d, s \to K^+$

NNPDF3.1 + MAPFF1.0 at **NNLO**

N³LL perturbative accuracy

Total 96 parameters

N = 2031 pts.

χ^2/N = 1.08

cuts

$\langle Q \rangle > 1.4$ GeV

$0.2 < z < 0.7$

Drell-Yan $q_T < 0.2\,Q$

SIDIS

$P_{hT} < \min\left[\min[0.2\,Q,\, 0.5\,Qz] + 0.3\,\text{GeV},\, zQ\right]$

correlation matrix

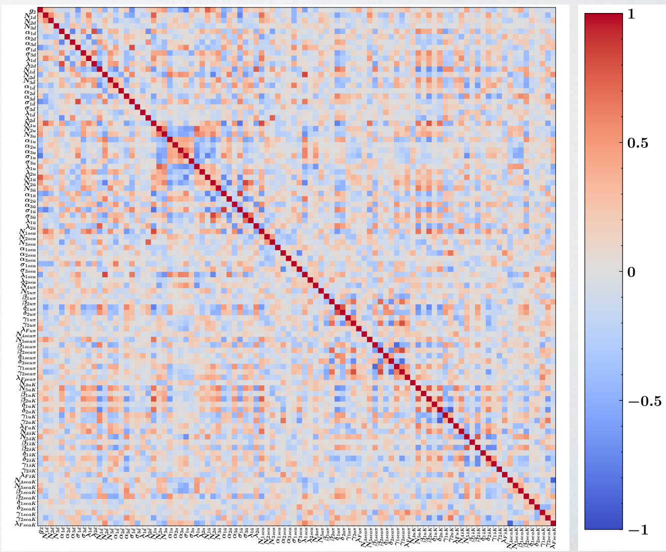

"Normalized" MAPTMD24 TMD PDFs

$$\frac{f_1(x, k_T; Q)}{f_1(x, 0; Q)}$$

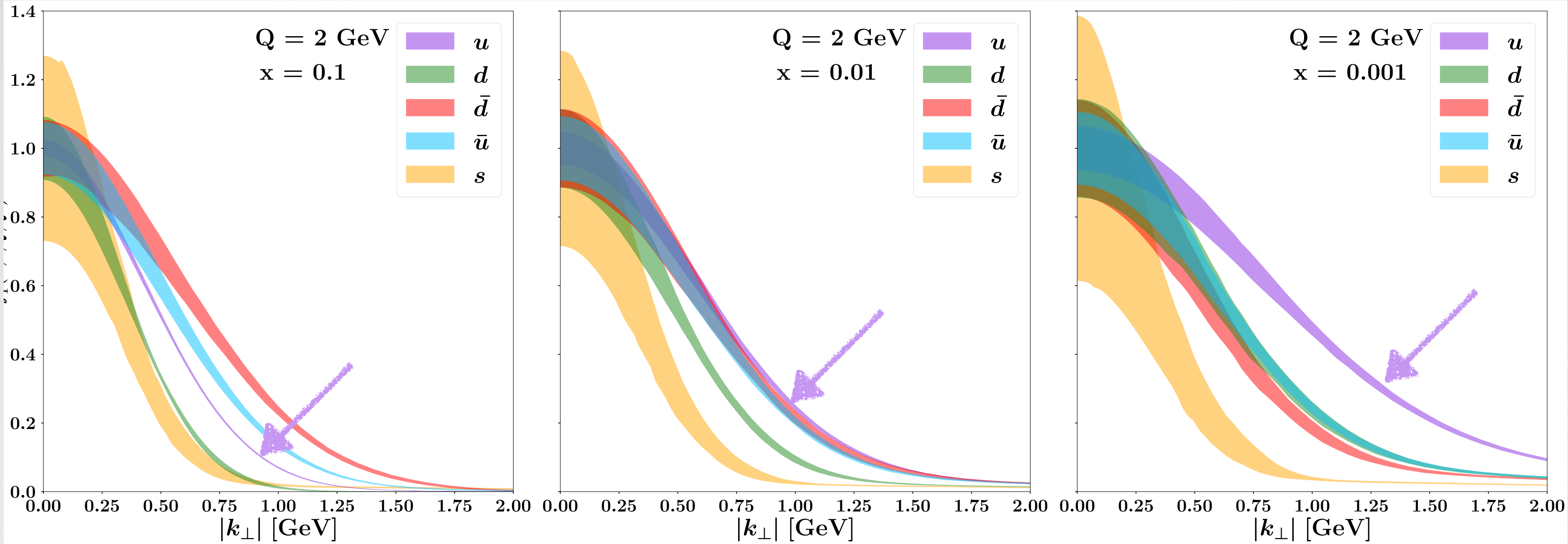

th. error band =
68% of all replicas

- very different k_T behavior
- it changes with x

MAPTMDNN: TMDs with Neural Networks

Bacchetta et al. (MAP), arXiv:2502.04166

same settings as MAPTMD22 & MAPTMD24
but limited to Drell-Yan data

$$f_{\mathrm{NP}}(x, b_T) = \frac{\mathbb{NN}(x, b_T)}{\mathbb{NN}(x, 0)}$$

$\mathbb{NN}$ architecture

[2, 10, 1]

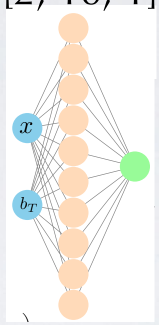

activation $\sigma(z) = \frac{1}{2}\left(1 + \frac{z}{1+|z|}\right)$

N³LL perturbative accuracy

Total 41+1 parameters

N = 482 pts. χ²/N = 0.97

avoid overfitting

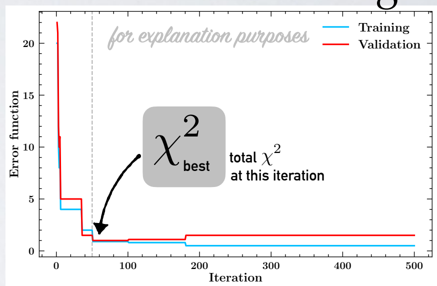

50%
50%

MAPTMDNN: TMDs with Neural Networks

Bacchetta et al. (MAP), arXiv:2502.04166

same settings as MAPTMD22 & MAPTMD24
but limited to Drell-Yan data

$$f_{NP}(x, b_T) = \frac{\mathbb{NN}(x, b_T)}{\mathbb{NN}(x,0)}$$

$\mathbb{NN}$ architecture

[2, 10, 1]

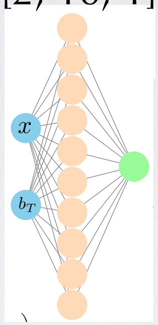

activation $\sigma(z) = \frac{1}{2}\left(1 + \frac{z}{1+|z|}\right)$

N^3LL perturbative accuracy

Total 41+1 parameters

N = 482 pts. $\chi^2/N = 0.97$

avoid overfitting

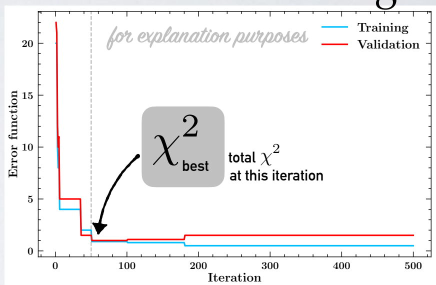

50%
50%

Neural Networks perform better than MAPTMD22 limited to Drell-Yan (**MAP22DY**), particularly on the most precise ATLAS data: $\chi^2 = 3.51 \rightarrow 1.38$

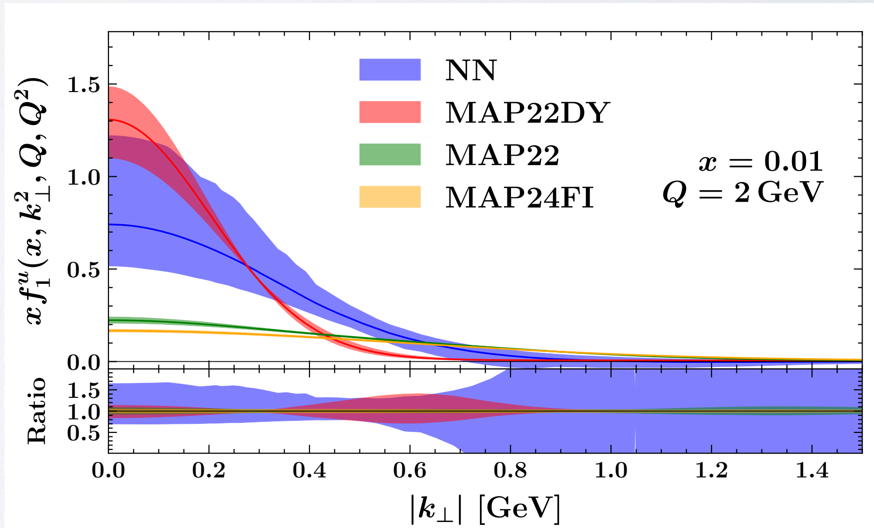

MAPTMDNN: TMDs with Neural Networks

Bacchetta et al. (MAP), arXiv:2502.04166

same settings as MAPTMD22 & MAPTMD24
but limited to Drell-Yan data

$$f_{NP}(x, b_T) = \frac{\mathbb{NN}(x, b_T)}{\mathbb{NN}(x, 0)}$$

$\mathbb{NN}$ architecture

[2, 10, 1]

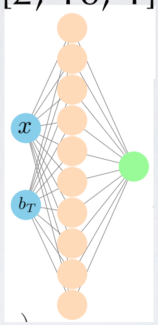

activation $\sigma(z) = \frac{1}{2}\left(1 + \frac{z}{1+|z|}\right)$

avoid overfitting

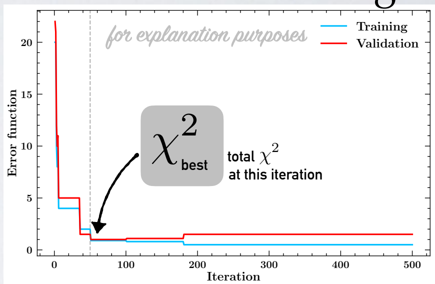

50%
50%

N³LL perturbative accuracy

Total 41+1 parameters

N = 482 pts. χ²/N = 0.97

Neural Networks perform better than MAPTMD22 limited to Drell-Yan (**MAP22DY**), particularly on the most precise ATLAS data: $\chi^2 = 3.51 \rightarrow 1.38$

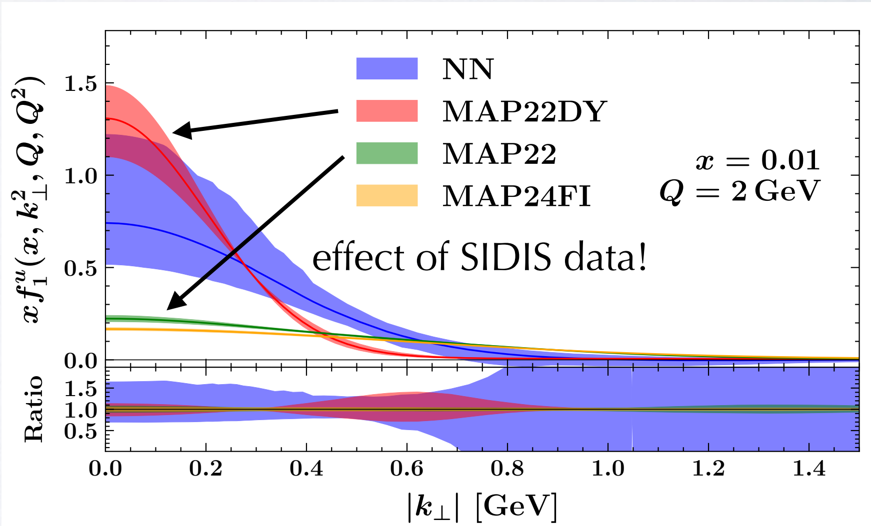

MAPTMDNN: TMDs with Neural Networks

Bacchetta et al. (MAP), arXiv:2502.04166

same settings as MAPTMD22 & MAPTMD24
but limited to Drell-Yan data

$$f_{NP}(x, b_T) = \frac{\mathbb{NN}(x, b_T)}{\mathbb{NN}(x, 0)}$$

$\mathbb{NN}$ architecture

[2, 10, 1]

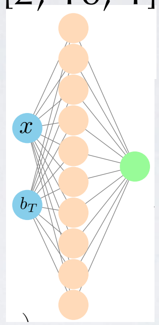

activation $\sigma(z) = \frac{1}{2}\left(1 + \frac{z}{1+|z|}\right)$

N³LL perturbative accuracy

Total 41+1 parameters

N = 482 pts. χ²/N = 0.97

avoid overfitting

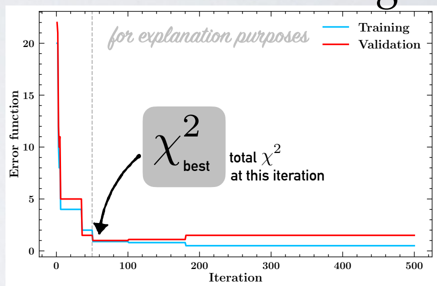

50%
50%

Neural Networks perform better than MAPTMD22 limited to Drell-Yan (**MAP22DY**), particularly on the most precise ATLAS data: $\chi^2 = 3.51 \rightarrow 1.38$

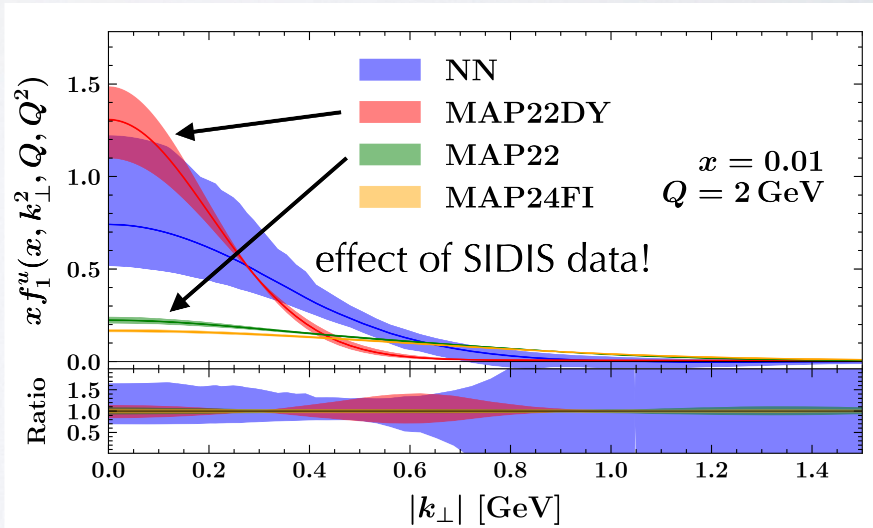

closure test - level 0 ✔

- generate pseudodata with known DWS model and real-data uncertainties
  Davies et al., N.P. **B256** (85)
- reproduce result with NN

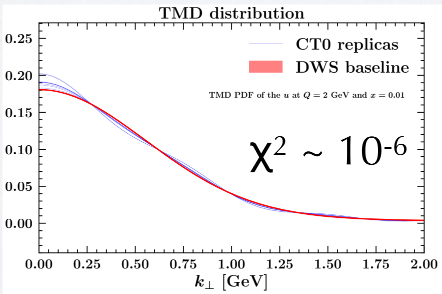

MAPTMDNN: TMDs with Neural Networks

Bacchetta et al. (MAP), arXiv:2502.04166

same settings as MAPTMD22 & MAPTMD24
but limited to Drell-Yan data

$$f_{NP}(x, b_T) = \frac{\mathbb{NN}(x, b_T)}{\mathbb{NN}(x, 0)}$$

$\mathbb{NN}$ architecture

[2, 10, 1]

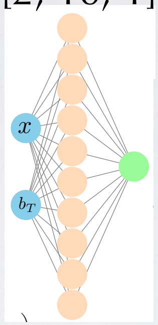

activation $\sigma(z) = \frac{1}{2}\left(1 + \frac{z}{1+|z|}\right)$

N³LL perturbative accuracy

Total 41+1 parameters

N = 482 pts. χ²/N = 0.97

avoid overfitting

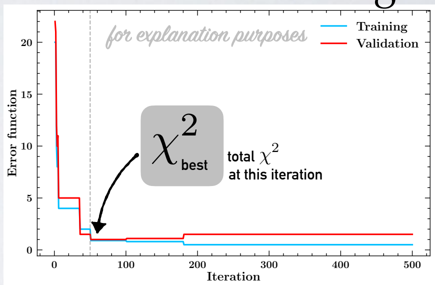

50%
50%

NN PDFs → NN TMDs !

Neural Networks perform better than MAPTMD22 limited to Drell-Yan (**MAP22DY**), particularly on the most precise ATLAS data: $\chi^2 = 3.51 \rightarrow 1.38$

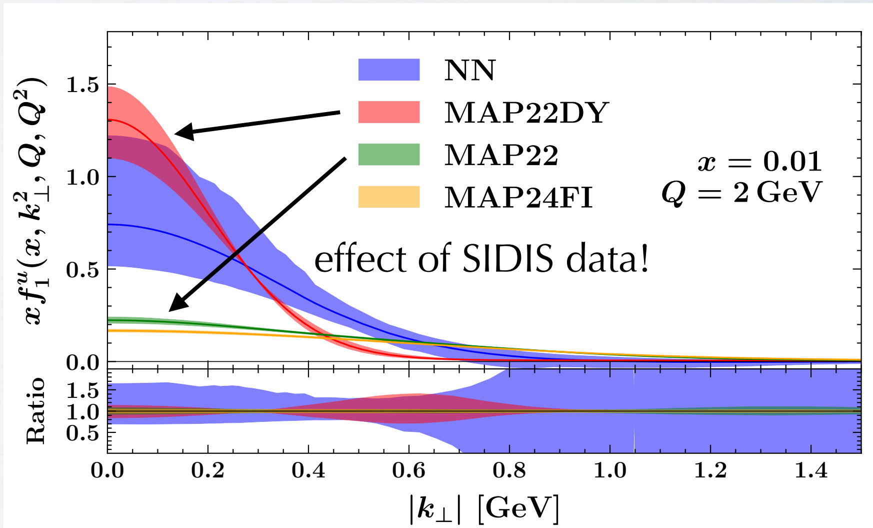

closure test - level 0 ✔

- generate pseudodata with known DWS model and real-data uncertainties
  Davies et al., N.P. **B256** (85)
- reproduce result with NN

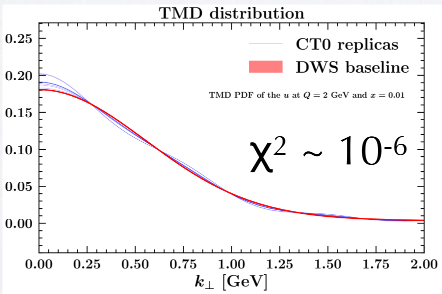

Comparison among most recent extractions

TMD PDFs at Q=10 GeV

Moos et al., arXiv:2503.11201

ART25, MAP24 — global fits

ART23, MAPNN — only Drell-Yan

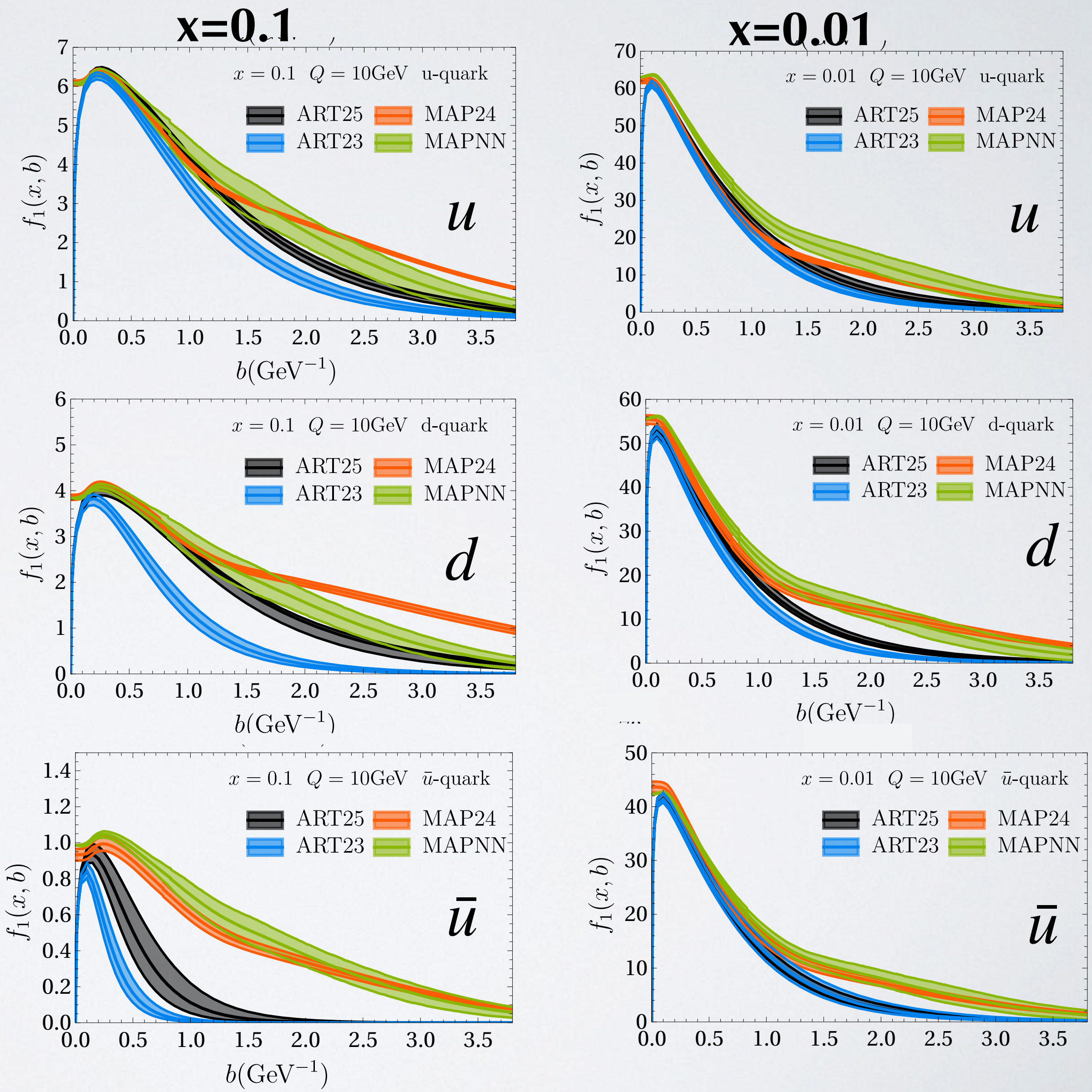

Comparison among most recent extractions

TMD PDFs at Q=10 GeV

Moos et al., arXiv:2503.11201

effect of $b_{\min}$ prescription

$$b_{\min} = \frac{2e^{-\gamma_E}}{\mu_f} \longleftarrow b_*(b_T) \longrightarrow b_{\max} = 2e^{-\gamma_E}$$

$$\mu_f \geq \mu_{b_*} = \frac{2e^{-\gamma_E}}{b_*(b_T)} \geq 1$$

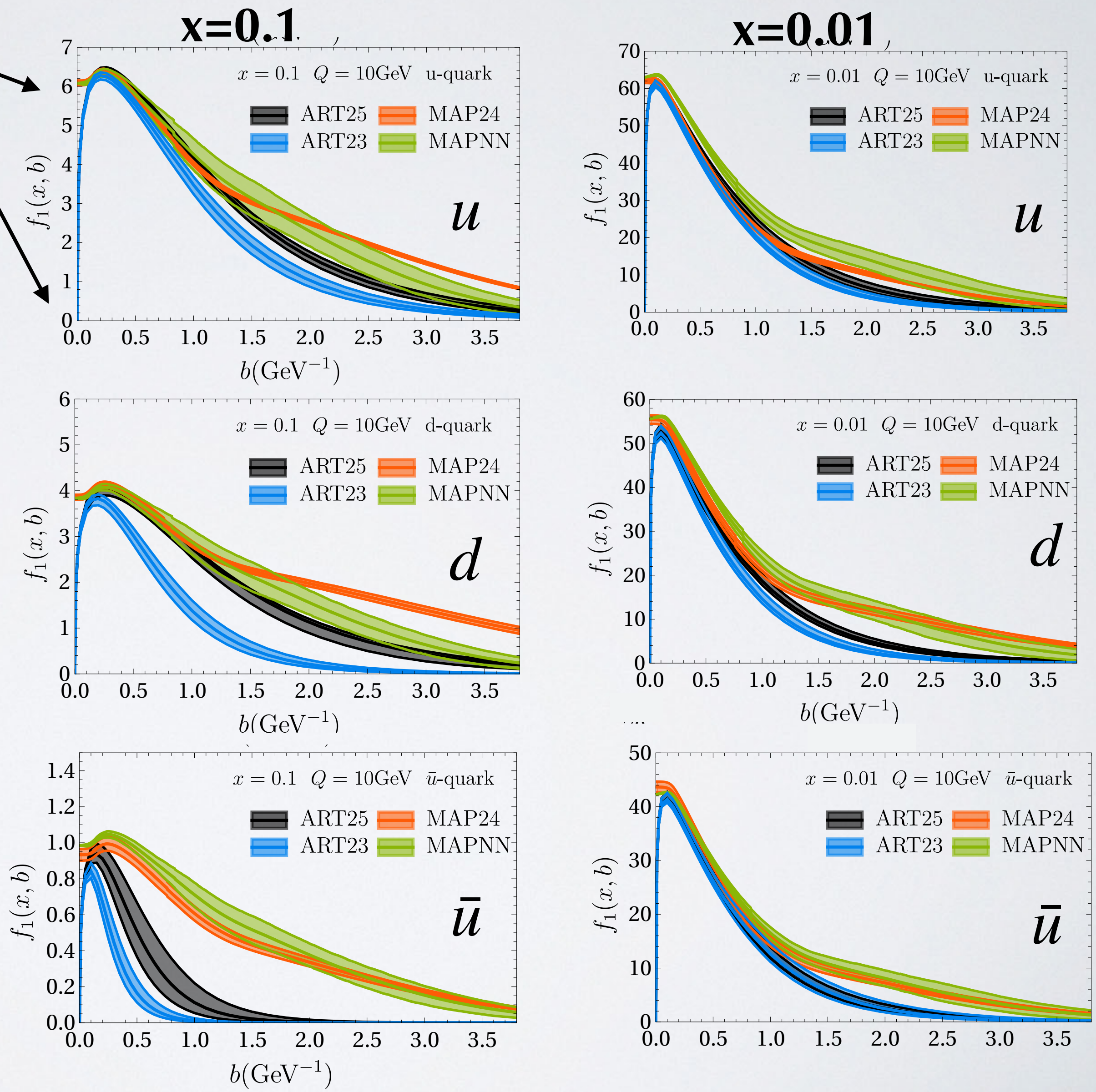

$$\tilde{f}_1(x,0) = \int d\mathbf{k}_T\, f_1(x,\mathbf{k}_T) = f_1(x)$$

$$= 0$$

?

Comparison among most recent extractions

TMD FFs at z=0.3 , Q=10 GeV

Moos et al., arXiv:2503.11201

all global fits

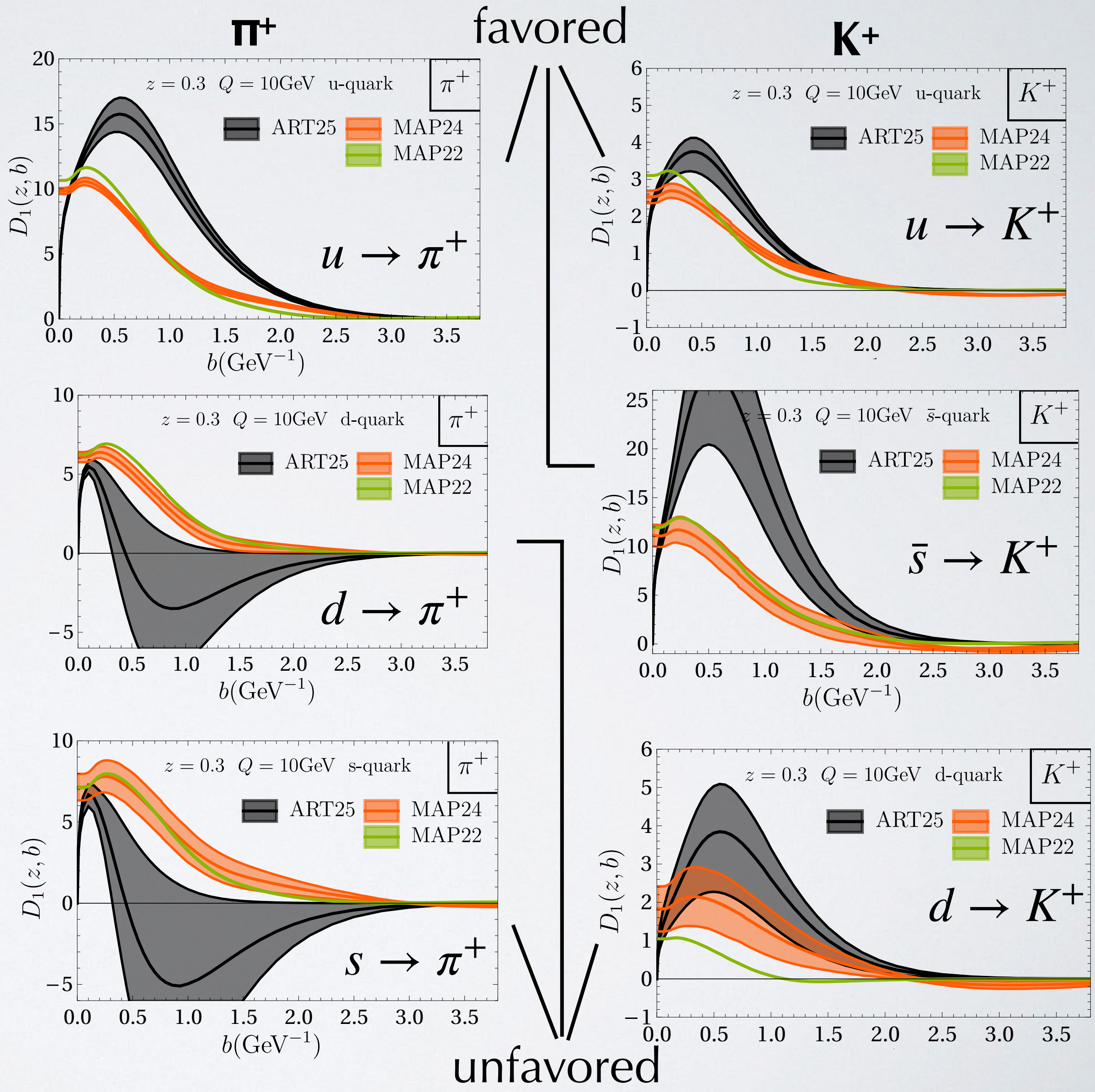

Comparison among most recent extractions

TMD FFs at z=0.3 , Q=10 GeV

Moos et al., arXiv:2503.11201

$$D_1(z, b_T) < 0$$

$$\int d\mathbf{b}_T \, e^{-i\mathbf{k}_T \cdot \mathbf{b}_T} D_1(z, b_T) = D_1(z, \mathbf{k}_T) > 0$$

?

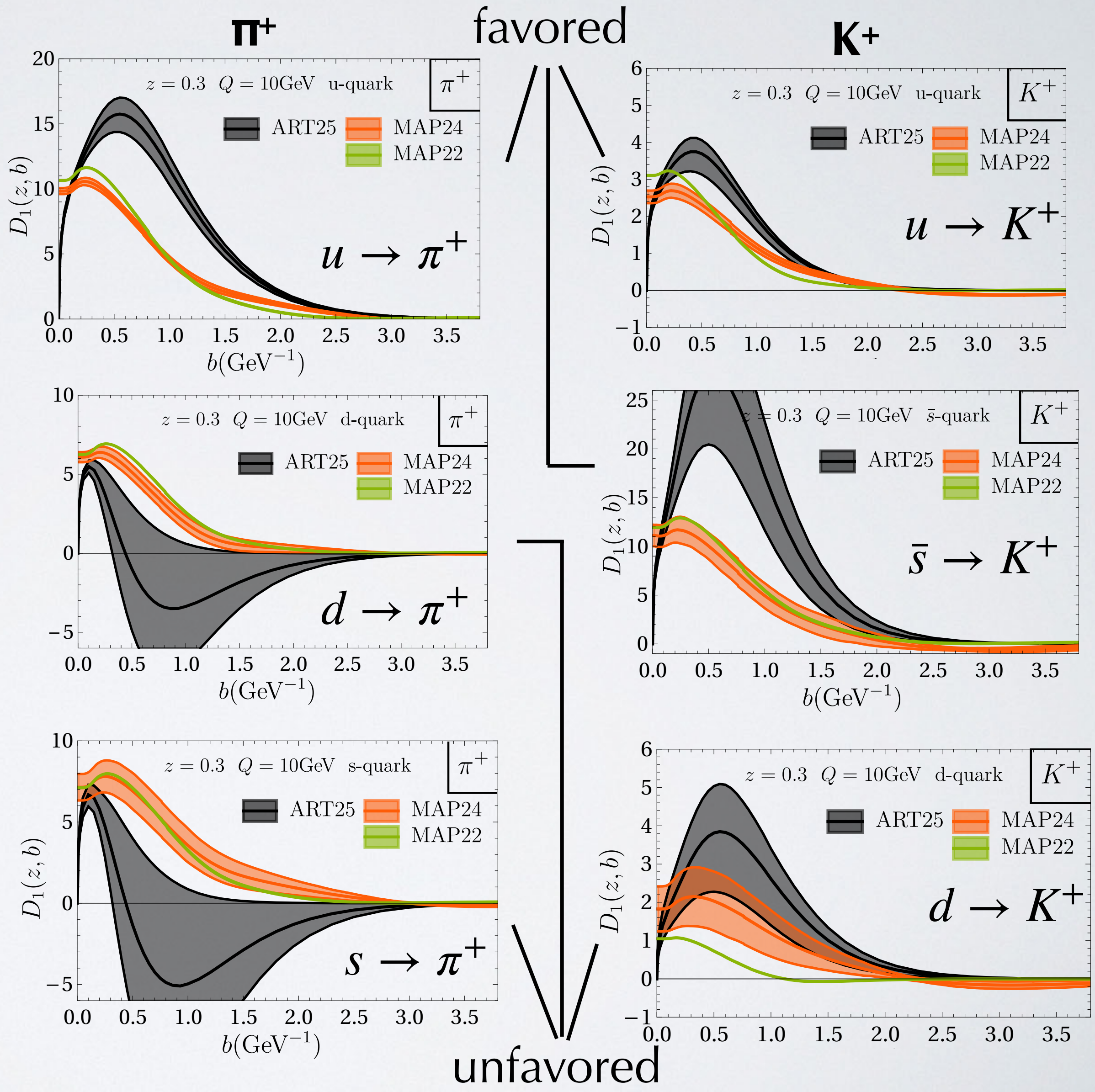

MAPTMD22: validity of TMD region ?

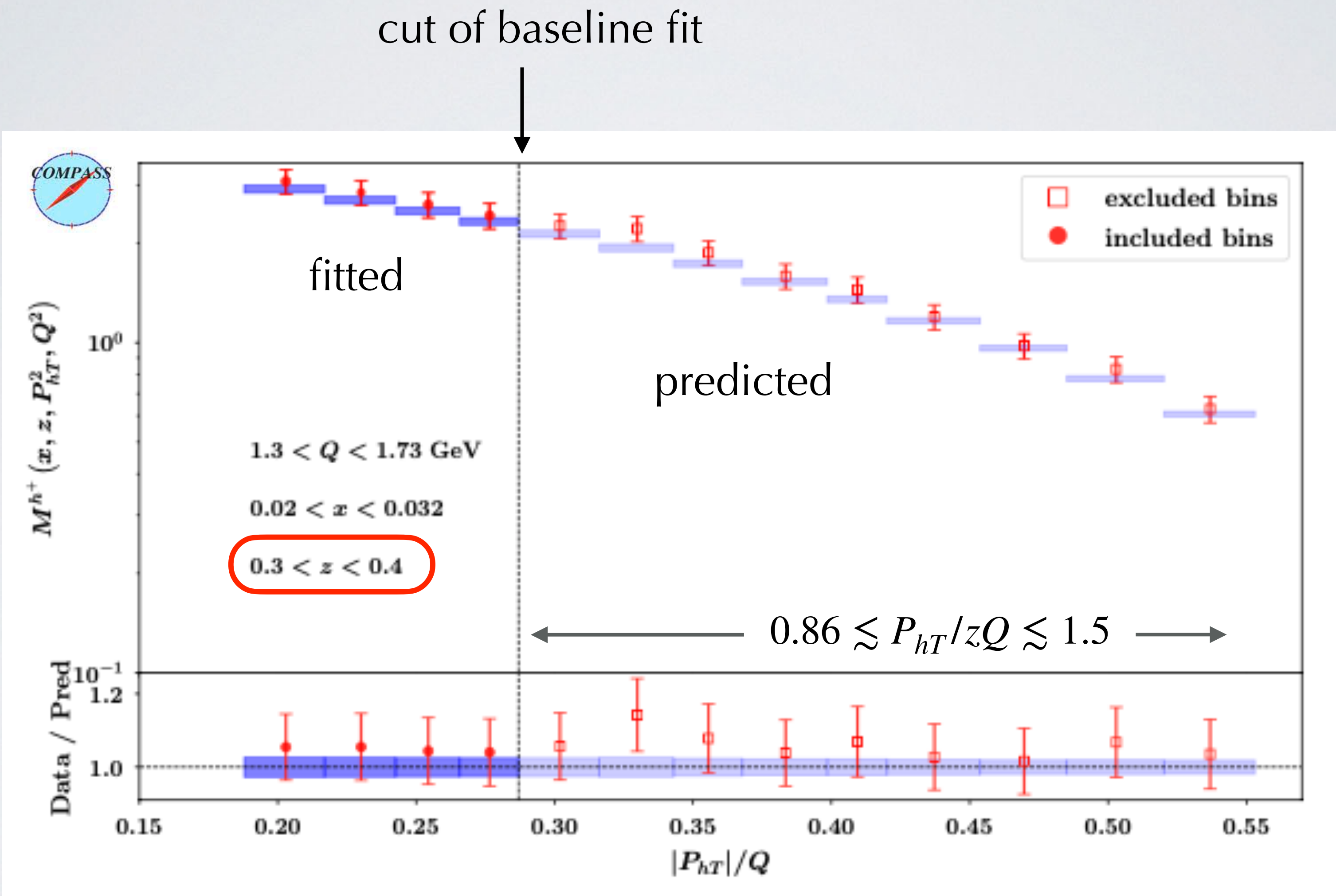

?

validity of TMD factorization seems to extend well beyond $P_{hT}/z << Q$!

Collins-Soper evolution kernel

universal flavor-independent
drives evolution in rapidity ζ

$K(b_*, \mu_b)$ + $g_K(b_T)$ fitted to data; input from lattice

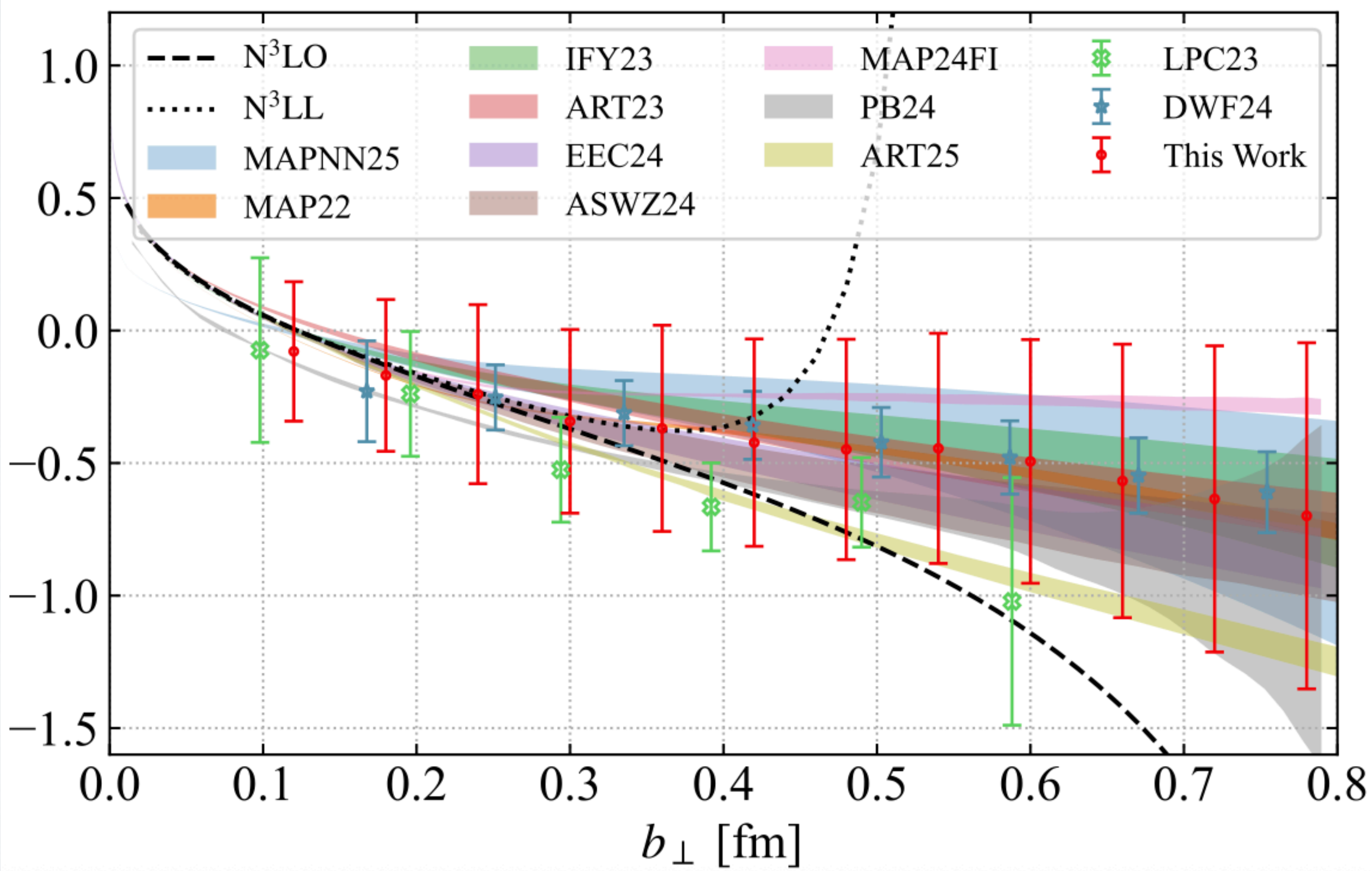

Bollweg et al., arXiv:2504.04625

(see talk by P. Shanahan and S.Mukherjee)

Lattice

DWF24 Bollweg et al., arXiv:2403.00664

LPC23 Chu et al. (LPC), arXiv:2306.06488

ASWZ24 Avkhadiev et al., arXiv:2402.06725

Pheno

IFY23 (ResBos)
Isaacson et al., arXiv:2311.09916

EEC24 Kang et al., arXiv:2410.21435

PB24 Martinez et al., arXiv:2412.21116

+ MAPTMD-22, -24, -NN

+ ART-23, -25

pQCD

N³LL Vladimirov, arXiv:1610.05791

N³LO Li&Zhu, arXiv:1604.01404

Ratio of different flavors from lattice

Bollweg et al., arXiv:2505.18430

$$\frac{f_1^{u_v}(x, b_T; \mu, \zeta)}{f_1^{d_v}(x, b_T; \mu, \zeta)}$$

$$\mu = \sqrt{\zeta} = 1.62 \text{ GeV}$$

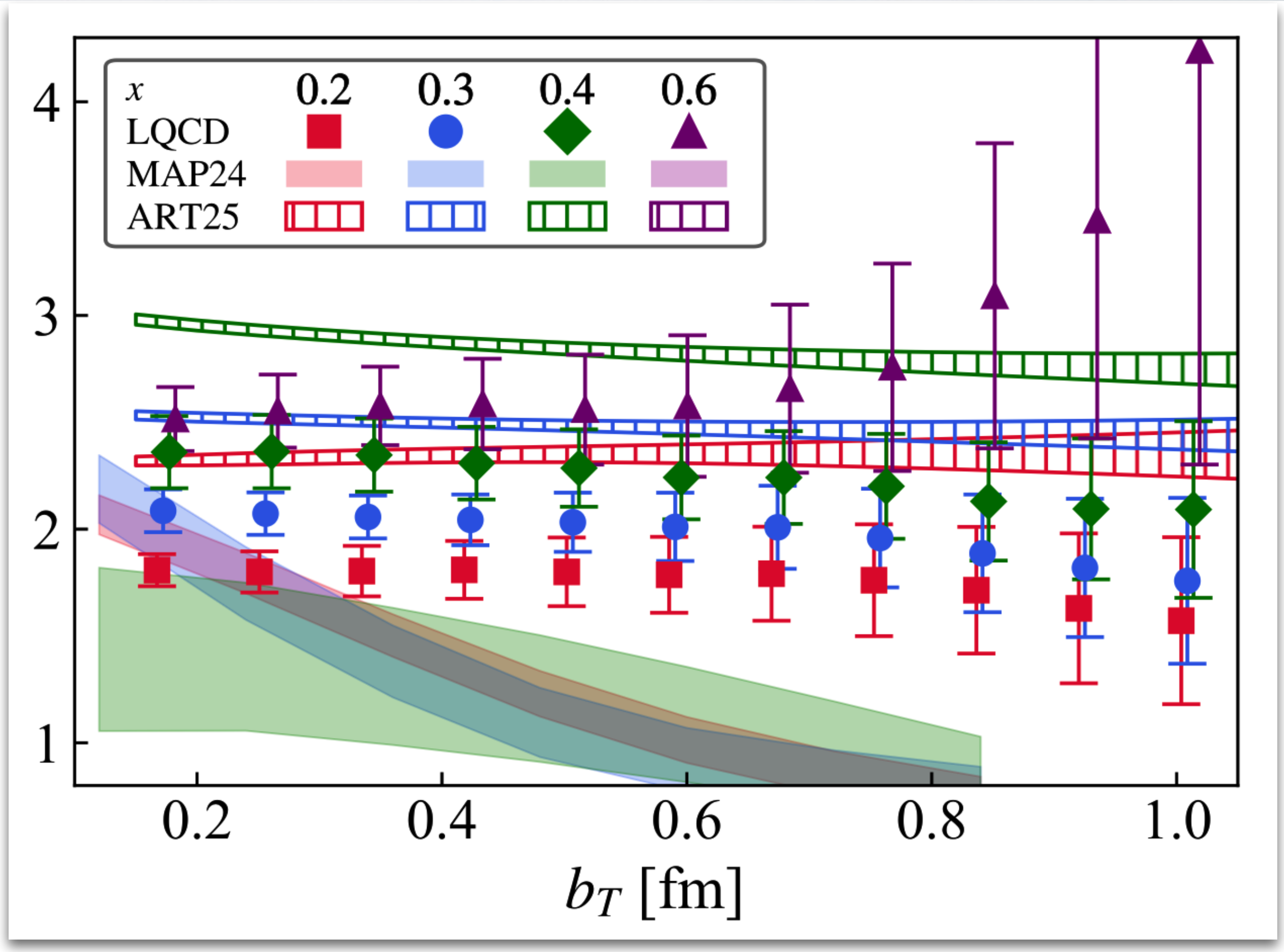

(see talk by S.Mukherjee)

Ratio of different flavors from lattice

Bollweg et al., arXiv:2505.18430

$$\frac{f_1^{u_v}(x, b_T; \mu, \zeta)}{f_1^{d_v}(x, b_T; \mu, \zeta)}$$

$\mu = \sqrt{\zeta} = 1.62$ GeV

?

at $b_T = 0$, ratio is given by collinear PDFs

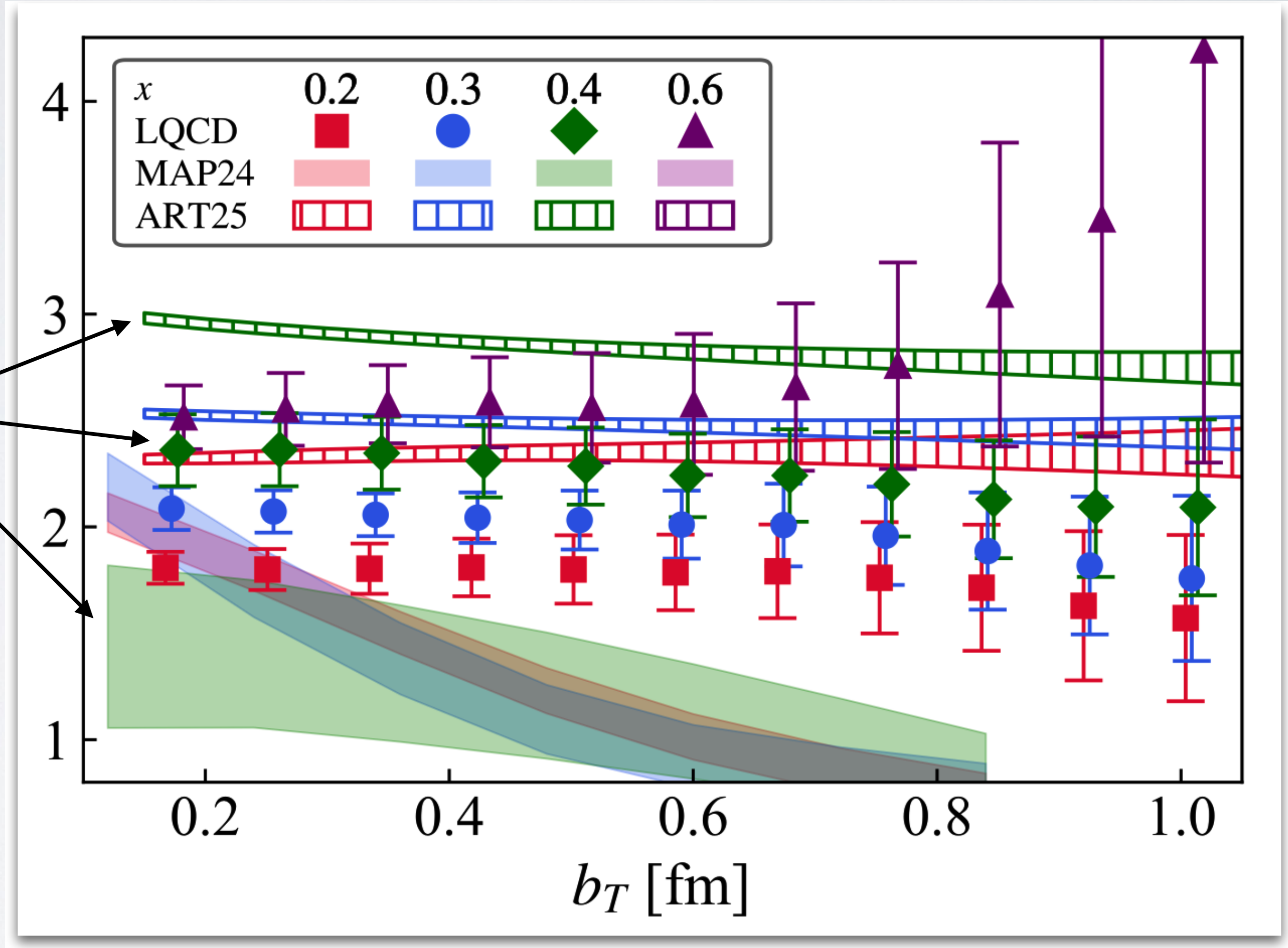

(see talk by S.Mukherjee)

Phase space for processes with factorization

Drell Yan { fixed target / collider

SIDIS

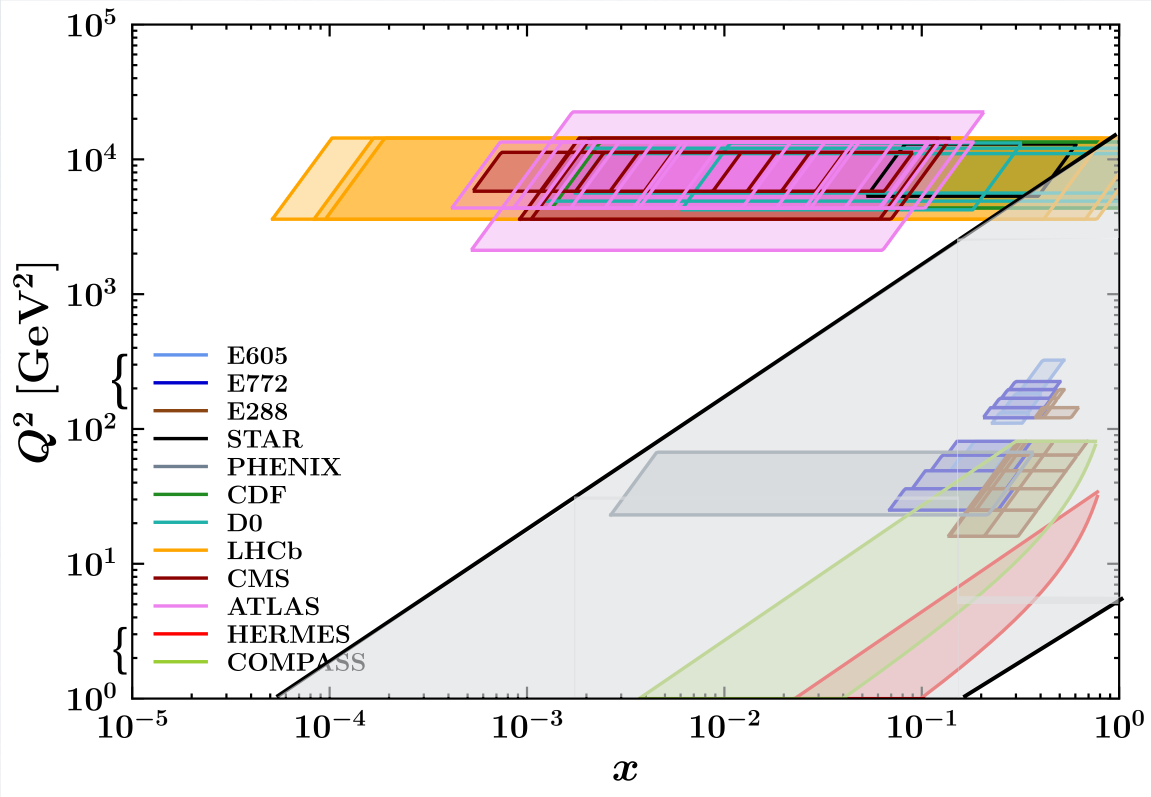

EIC coverage

The EIC impact at x=0.01

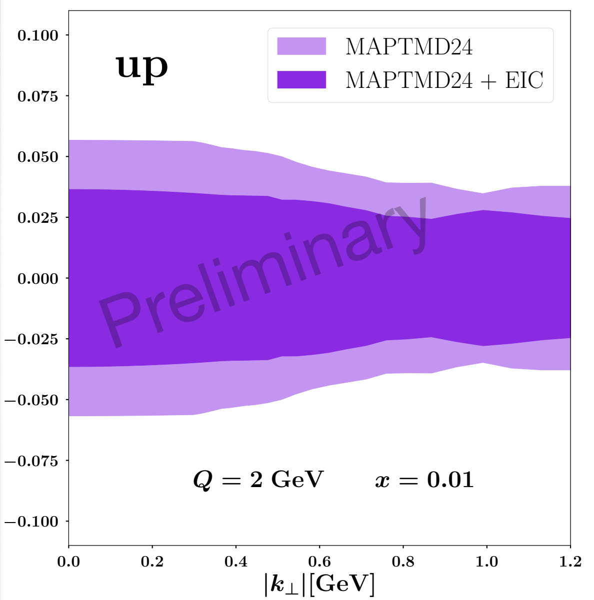

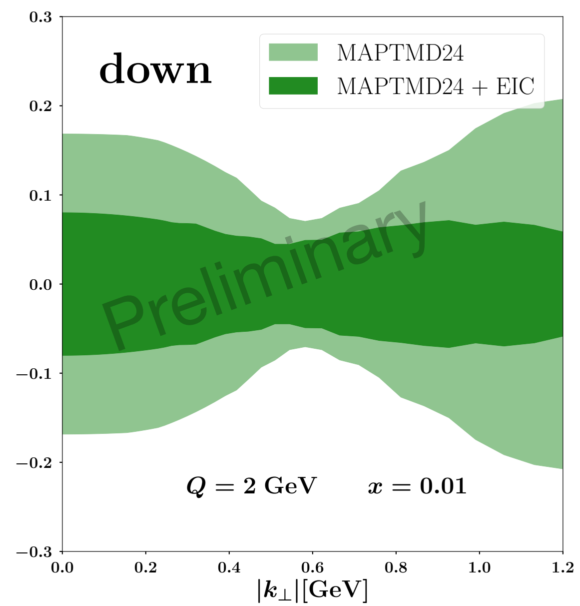

$$\frac{\mathrm{TMD}^q - \langle \mathrm{TMD}^q \rangle}{\langle \mathrm{TMD}^q \rangle} \quad x=0.01$$

MAPTMD24	2031	
EIC	**# pts.**	**lumi [fb^{-1}]**
5x41	1273	2.85
10x100	1611	51.3
18x275	1648	10

(simulation campaign of May 2024 only π+ production)

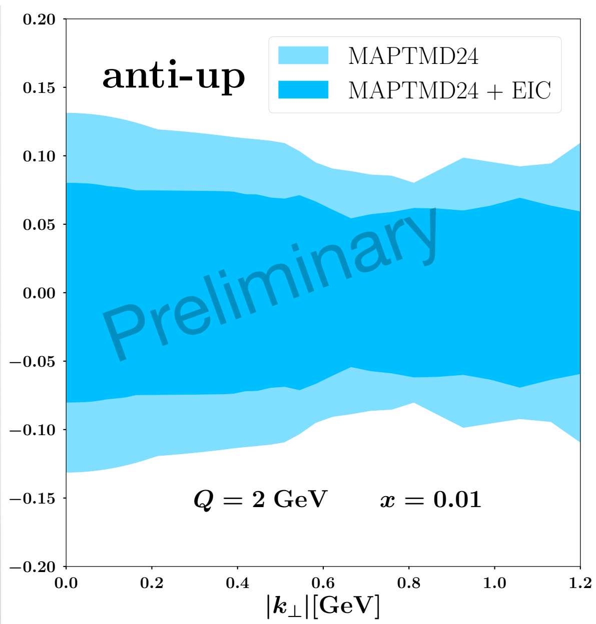

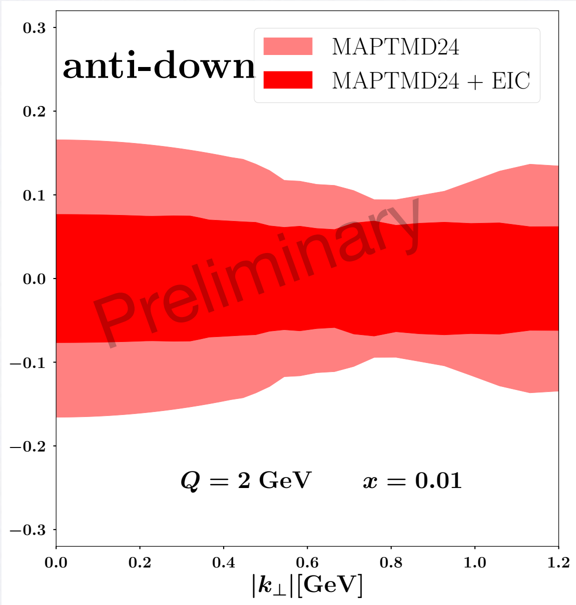

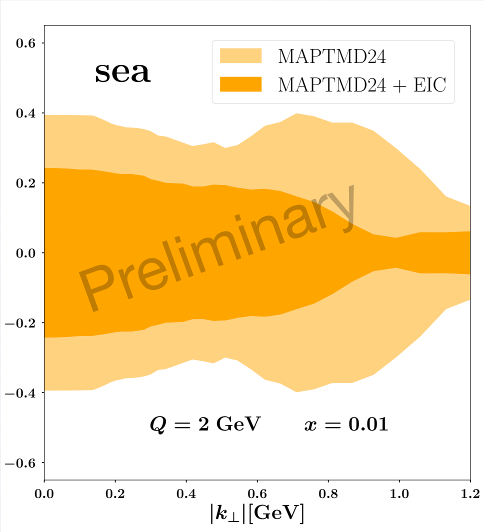

L. Rossi, Ph.D. Thesis

The EIC impact at x=0.001

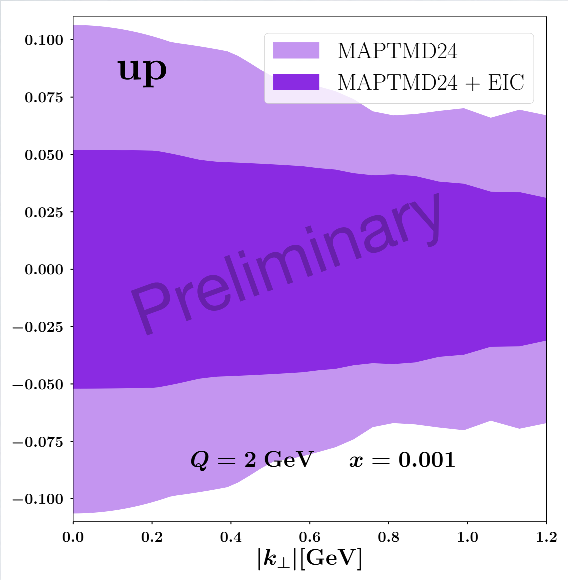

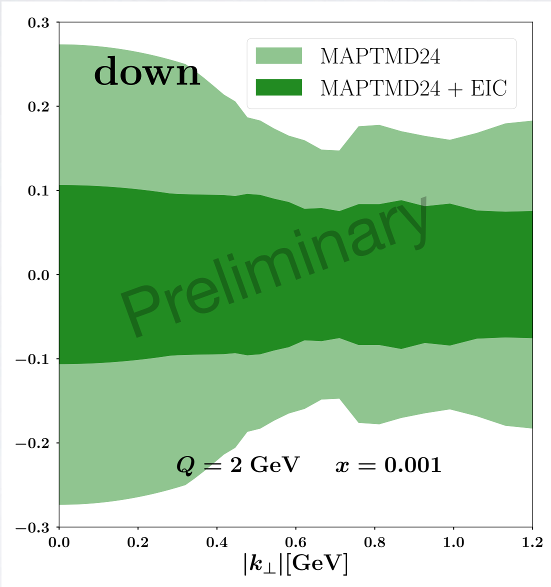

$$\frac{\text{TMD}^q - \langle \text{TMD}^q \rangle}{\langle \text{TMD}^q \rangle} \quad \mathbf{x=0.001}$$

MAPTMD24	2031	
EIC	**# pts.**	**lumi [fb^{-1}]**
5x41	1273	2.85
10x100	1611	51.3
18x275	1648	10

(simulation campaign of May 2024 only π+ production)

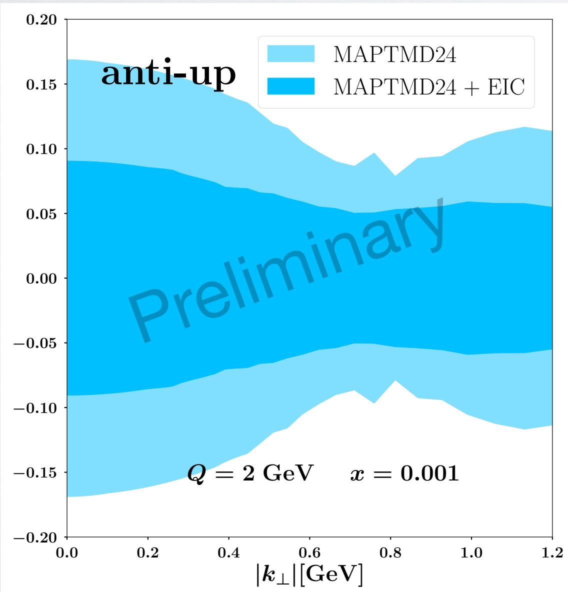

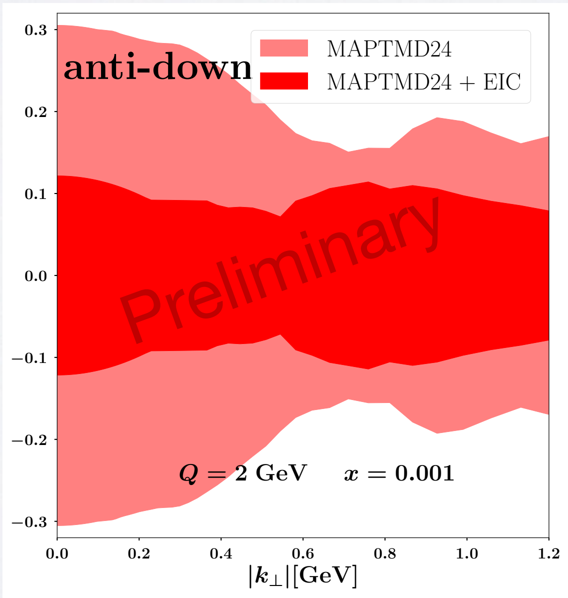

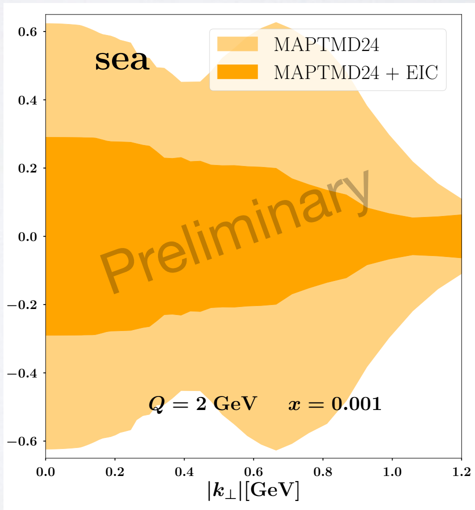

L. Rossi, Ph.D. Thesis

Early Science Conditions

ep Luminosity for Phase-1

High Divergence	Lumi per Fill (5 h)	Lumi per Year
5 GeV e x 250 GeV p	9.26 pb^{-1}	6.48 fb^{-1}
10 GeV e x 250 GeV p	13.12 pb^{-1}	9.18 fb^{-1}
5 GeV e x 130 GeV p	6.3 pb^{-1}	4.36 fb-1
10 GeV e x 130 GeV p	7.6 pb^{-1}	5.33 fb^{-1}

Low Divergence	Lumi per Fill (5 h)	Lumi per Year
5 GeV e x 250 GeV p	6.81 pb^{-1}	4.78 fb^{-1}
10 GeV e x 250 GeV p	8.8 pb^{-1}	6.19 fb^{-1}
5 GeV e x 130 GeV p	5.8 pb^{-1}	4.1 fb^{-1}
10 GeV e x 130 GeV p	7.1 pb^{-1}	4.95 fb^{-1}

Compare to HERA integrated luminosity 1992 – 2007: 0.6 fb^{-1}

Remember:
high divergence: higher lumi, but reduced acceptance for low forward particle p_T^{min}
low divergence: lower lumi, but increased acceptance for low forward particle p_T^{min}
→ important for exclusive processes

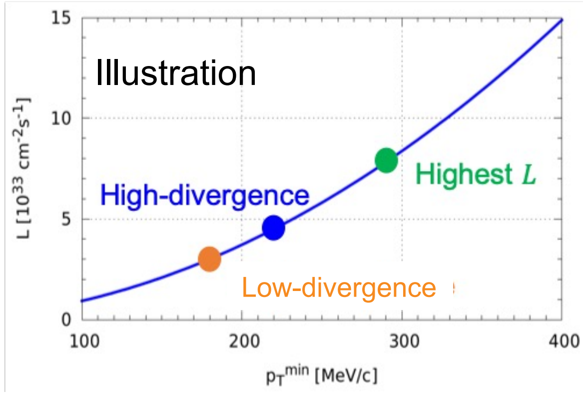

Early Science Conditions

ep Luminosity for Phase-1

High Divergence	Lumi per Fill (5 h)	Lumi per Year	Low Divergence	Lumi per Fill (5 h)	Lumi per Year
5 GeV e x 250 GeV p	9.26 pb^{-1}	6.48 fb^{-1}	5 GeV e x 250 GeV p	6.81 pb^{-1}	4.78 fb^{-1}
10 GeV e x 250 GeV p	13.12 pb^{-1}	9.18 fb^{-1}	10 GeV e x 250 GeV p	8.8 pb^{-1}	6.19 fb^{-1}
5 GeV e x 130 GeV p	6.3 pb^{-1}	4.36 fb-1	5 GeV e x 130 GeV p	5.8 pb^{-1}	4.1 fb^{-1}
10 GeV e x 130 GeV p	7.6 pb^{-1}	5.33 fb^{-1}	10 GeV e x 130 GeV p	7.1 pb^{-1}	4.95 fb^{-1}

Compare to HERA integrated luminosity 1992 – 2007: 0.6 fb^{-1}

Remember:
high divergence: higher lumi, but reduced acceptance for low forward particle p_T^{min}
low divergence: lower lumi, but increased acceptance for low forward particle p_T^{min}
→ important for exclusive processes

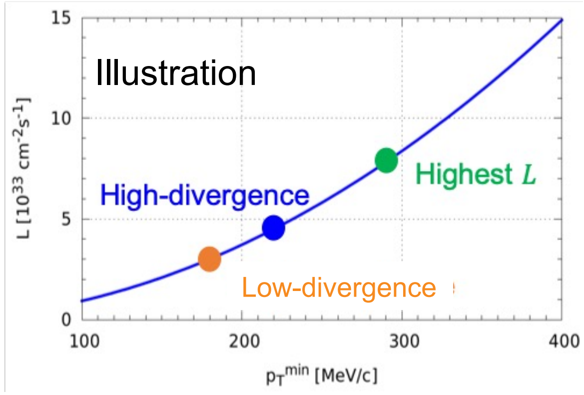

EIC impact in Early Science Conditions

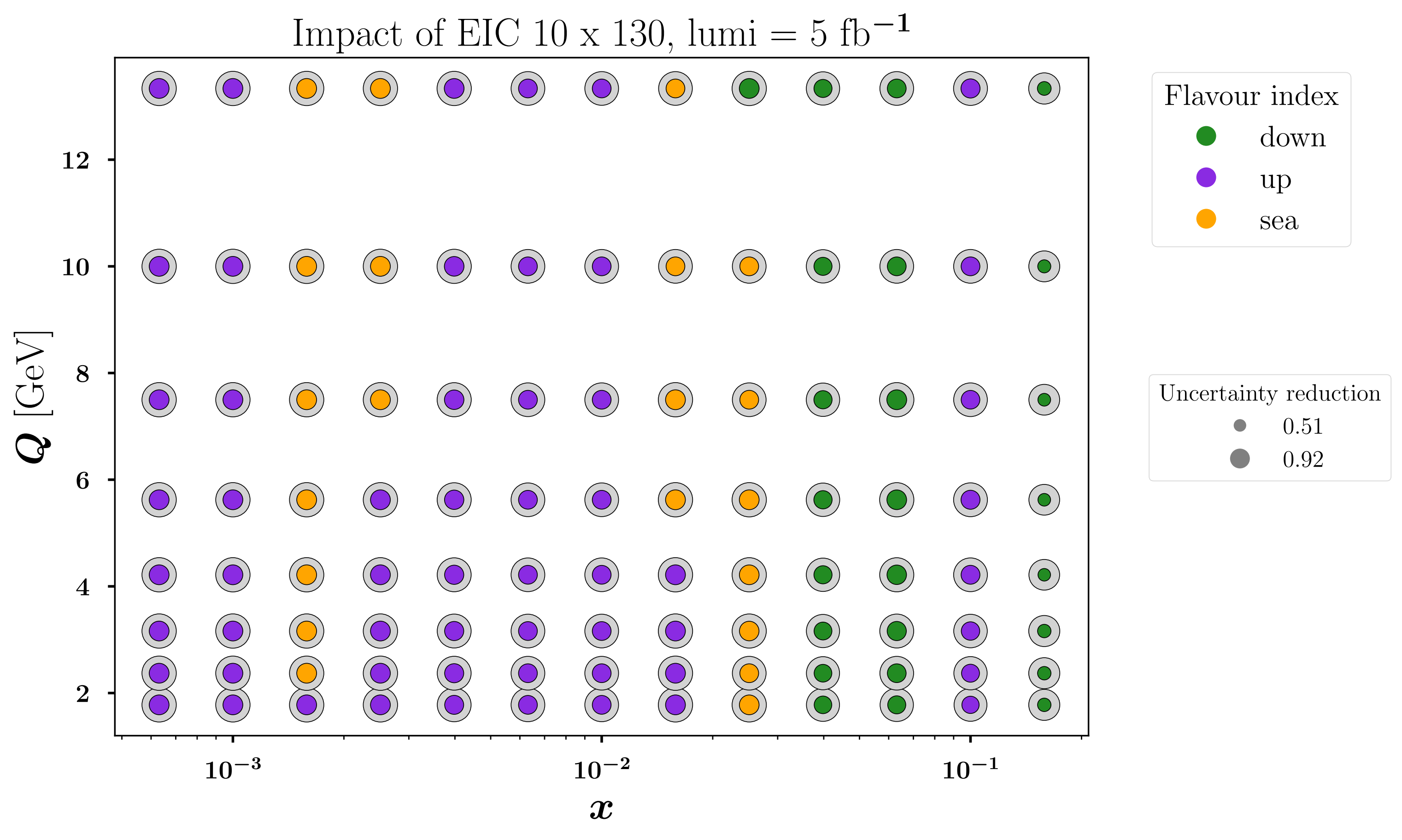

For each (x,Q^2) bin:

- from MAPTMD24, max. uncertainty of $f_1^q(x,k_T;Q)$ over all k_T and all flavors q
- including EIC pseudodata, color code indicates the flavor with max. reduction in uncertainty over all k_T

EIC impact in Early Science Conditions

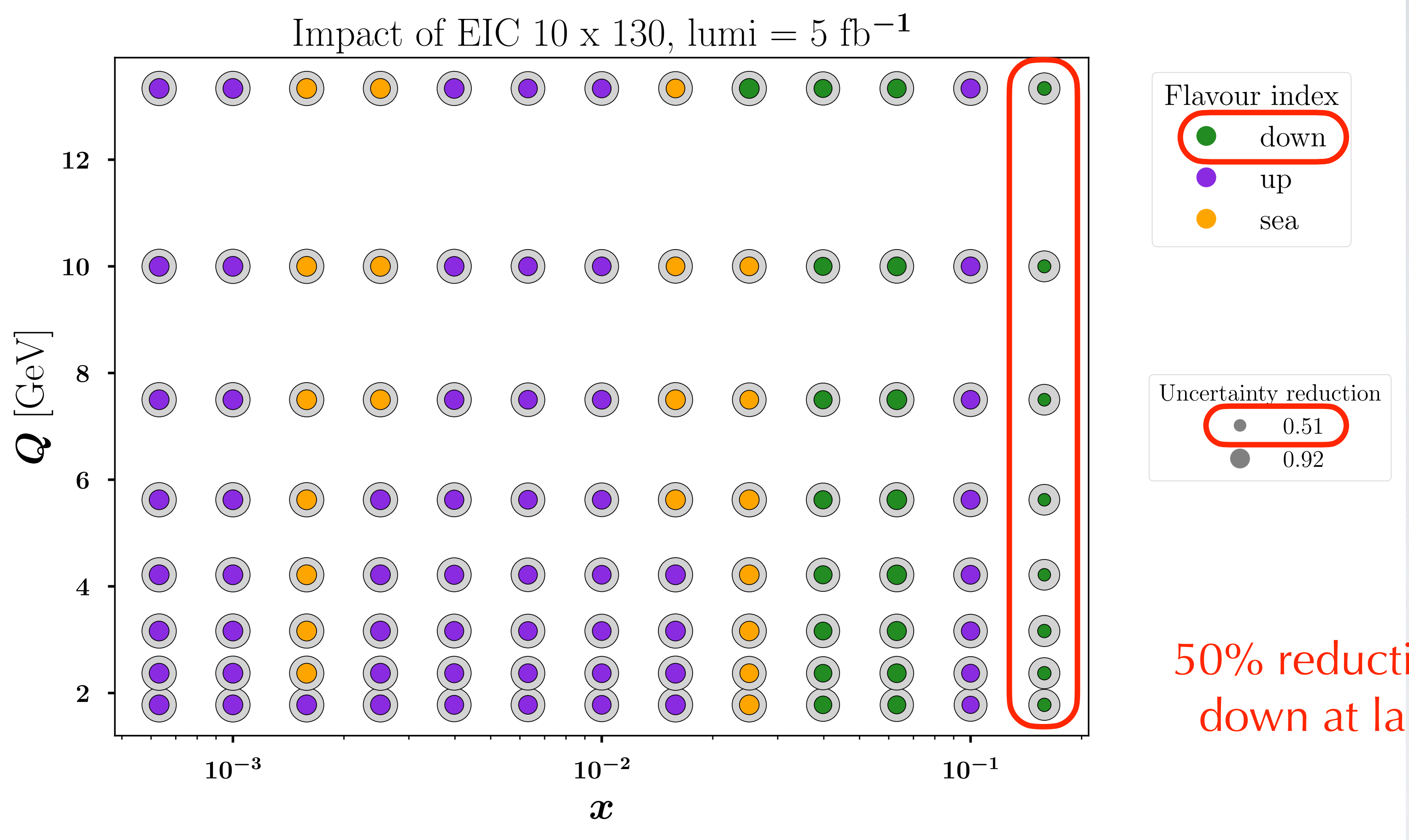

50% reduction on down at large x

For each (x,Q²) bin:

- from MAPTMD24, max. uncertainty of $f_1^q(x,k_T;Q)$ over all k_T and all flavors q
- including EIC pseudodata, color code indicates the flavor with max. reduction in uncertainty over all k_T

The EIC impact with 10x130 at x=0.16

MAPTMD24 2031

EIC	**# pts.**	**lumi [fb-1]**
10x130	~1620	5

(early Science conditions, only π+ production)

$$\frac{\text{TMD}^q - \langle\text{TMD}^q\rangle}{\langle\text{TMD}^q\rangle}$$

x=0.16, Q=1.77 GeV

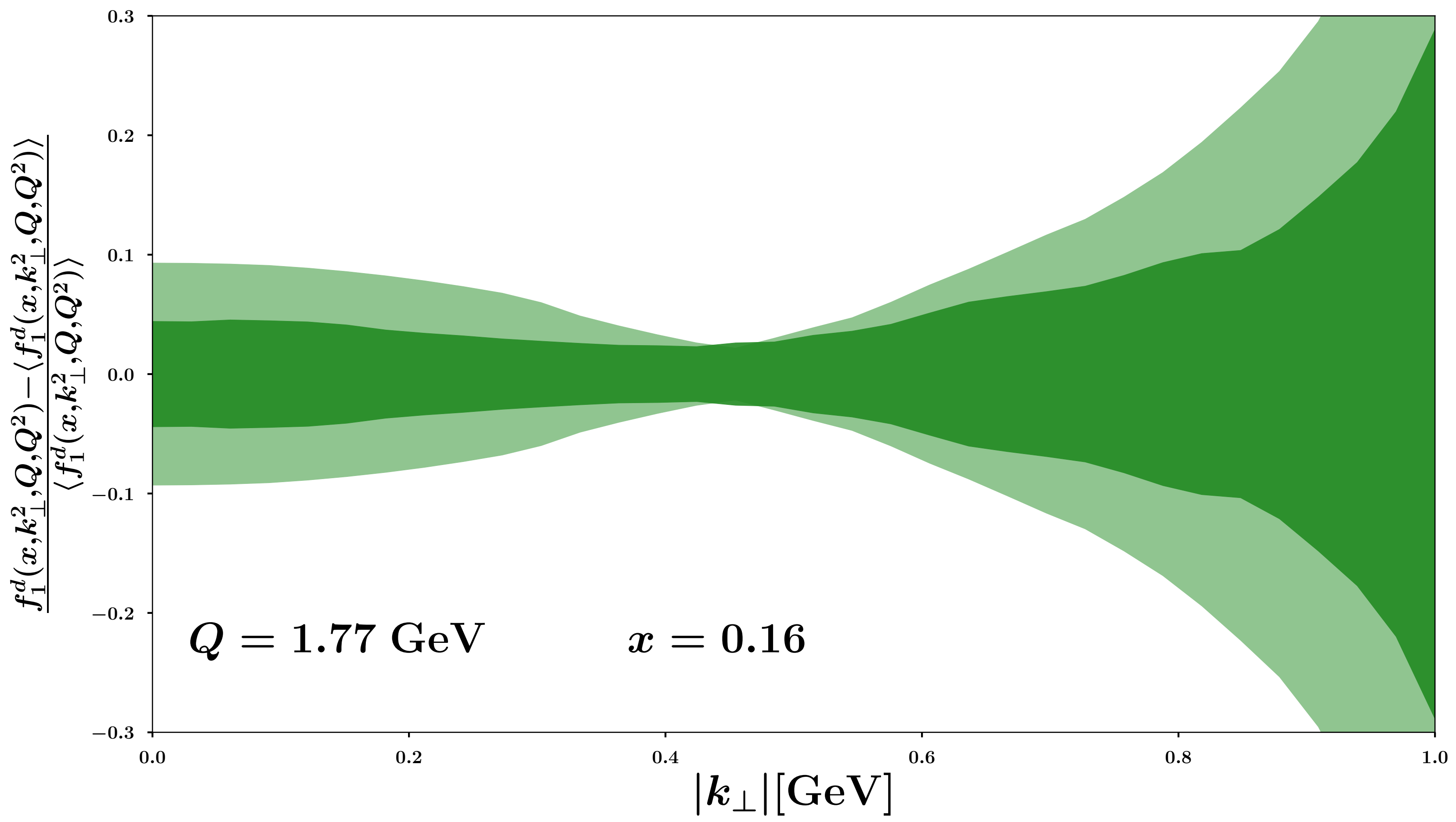

courtesy L. Rossi

Helicity TMD PDF

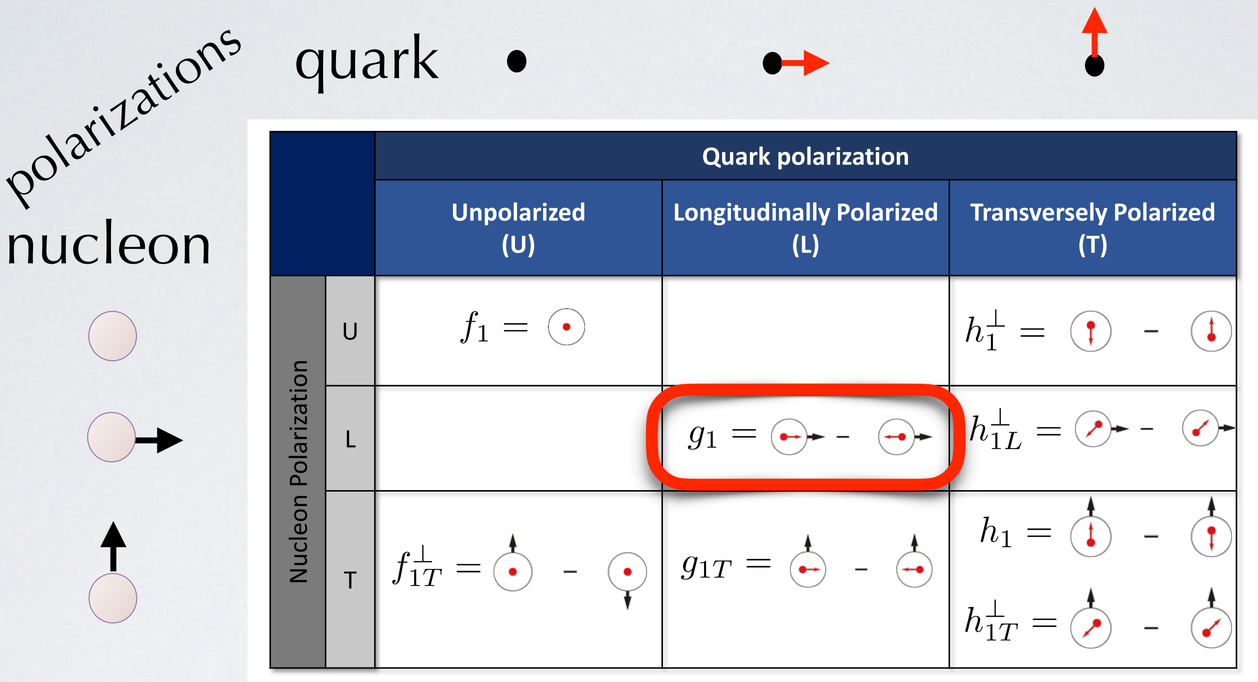

- How polarization of quarks distorts their k_T ?
- Do quarks with spin parallel to proton spin have larger / smaller k_T than those with spin antiparallel ?

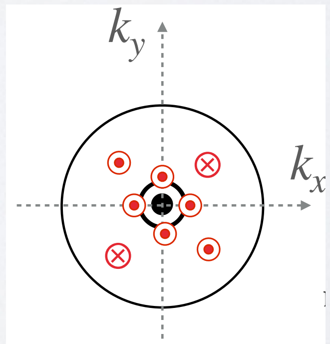

Double Spin Asymmetry

$$A_1(x, z, |\mathbf{P}_{hT}|, Q) = \frac{d\sigma^{\rightarrow\leftarrow} - d\sigma^{\rightarrow\rightarrow} + d\sigma^{\leftarrow\rightarrow} - d\sigma^{\leftarrow\leftarrow}}{d\sigma^{\rightarrow\leftarrow} + d\sigma^{\rightarrow\rightarrow} + d\sigma^{\leftarrow\rightarrow} + d\sigma^{\leftarrow\leftarrow}}$$

$$= \frac{\sum_{i=q,\bar{q}} e_i^2 \int_0^\infty db_T^2\, J_0\left(b_T |\mathbf{P}_{hT}| / z\right) \tilde{g}_1^i(x, b_T^2; Q)\, \tilde{D}_1^{i\to h}(z, b_T^2; Q)}{\sum_{i=q,\bar{q}} e_i^2 \int_0^\infty db_T^2\, J_0\left(b_T |\mathbf{P}_{hT}| / z\right) \tilde{f}_1^i(x, b_T^2; Q)\, \tilde{D}_1^{i\to h}(z, b_T^2; Q)}$$

importance of consistency

	Accuracy	SIDIS	Drell-Yan	N of points	χ^2/N	Flavor dep.
MAPTMD22pol Bacchetta et al. (MAP) P.R.L. **134** (25) 121901	NNLL	✔	✘	291	1.09	✘
YLSZM Yang et al. (TNT) P.R.L. **134** (25) 121902	NNLL	✔	✘	253	0.74	✘

The MAPTMD22pol fit (in one slide)

TMD f_1 & D_1 from MAPTMD22

Bacchetta et al. (MAP) P.R.L. **134** (25) 121901

$$\tilde{g}_1^q(x, b_T^2; \mu_f, \zeta_f) = \text{Evo}\big[(\mu_f, \zeta_f) \leftarrow (\mu_i, \zeta_i)\big]\ \exp\Big[g_K(b_T)\ \log\Big(\sqrt{\zeta_f}/Q_0\Big)\Big]\ g_{\rm NP}(x, b_T)$$
$$\times \sum_i \Big[C_{qi}^g(x, b_T; \mu_i, \zeta_i) \otimes g_1^i(x, \mu_i)\Big]$$

same **Evo** and **g_K** from MAPTMD22; **C^g** up to **NLO** → **NNLL** max. pert. accuracy

$g_1(x,\mu_i)$ from NNPDFpol1.1 at **NLO**

Gutierrez-Reyes et al.,
P.L. **B769** (17) 84

YLSZM fit modifies $g_1(x,\mu_i)$ → breaking OPE formula!

$$\rightarrow \int d\mathbf{k}_T\, g_1(x, \mathbf{k}_T) \neq g_1(x) \quad \text{even at NLL!}$$

The MAPTMD22pol fit (in one slide)

Bacchetta et al. (MAP) P.R.L. **134** (25) 121901

TMD f_1 & D_1 from MAPTMD22

$$\tilde{g}_1^q(x, b_T^2; \mu_f, \zeta_f) = \mathrm{Evo}\big[(\mu_f, \zeta_f) \leftarrow (\mu_i, \zeta_i)\big] \; \exp\Big[g_K(b_T)\, \log\Big(\sqrt{\zeta_f}/Q_0\Big)\Big] \; g_{\mathrm{NP}}(x, b_T)$$
$$\times \sum_i \Big[C_{qi}^g(x, b_T; \mu_i, \zeta_i) \otimes g_1^i(x, \mu_i)\Big]$$

same **Evo** and **g_K** from MAPTMD22; **C^g** up to **NLO** → **NNLL** max. pert. accuracy

$g_1(x,\mu_i)$ from NNPDFpol1.1 at **NLO**

Gutierrez-Reyes et al., P.L. **B769** (17) 84

$$g_{\mathrm{NP}}(x, k_T^2) = f_{\mathrm{NP}}^{\mathrm{MAP22}}(x, k_T^2)\, \frac{e^{-k_T^2/w_1(x)}}{k_{\mathrm{norm}}(x)}$$

→ such that $\int d\mathbf{k}_T\, g_{\mathrm{NP}} = 1$

x-dep. width **$w_1(x)$** such that always $|g_1| \le f_1$ **ensure positivity**

(not granted in YLSZM fit)

At Q_0 $\quad \dfrac{|g_1(x, \mathbf{k}_T^2; Q_0)|}{f_1(x, \mathbf{k}_T^2; Q_0)} = \dfrac{|g_1(x; Q_0)|}{f_1(x; Q_0)}\, \dfrac{e^{-k_T^2/w_1(x)}}{k_{\mathrm{norm}}(x)} \le 1$

The MAPTMD22pol fit (in one slide)

Bacchetta et al. (MAP) P.R.L. **134** (25) 121901

TMD f_1 & D_1 from MAPTMD22

$$\tilde{g}_1^q(x, b_T^2; \mu_f, \zeta_f) = \text{Evo}\left[(\mu_f, \zeta_f) \leftarrow (\mu_i, \zeta_i)\right] \exp\left[g_K(b_T) \log\left(\sqrt{\zeta_f}/Q_0\right)\right] g_{NP}(x, b_T)$$
$$\times \sum_i \left[C_{qi}^g(x, b_T; \mu_i, \zeta_i) \otimes g_1^i(x, \mu_i)\right]$$

same **Evo** and **g_K** from MAPTMD22; **C^g** up to **NLO** → **NNLL** max. pert. accuracy

$g_1(x,\mu_i)$ from NNPDFpol1.1 at **NLO**

Gutierrez-Reyes et al., P.L. **B769** (17) 84

$$g_{NP}(x, k_T^2) = f_{NP}^{MAP22}(x, k_T^2) \frac{e^{-k_T^2 / w_1(x)}}{k_{norm}(x)}$$

→ such that $\int d\mathbf{k}_T \, g_{NP} = 1$

x-dep. width **$w_1(x)$** such that always $|g_1| \leq f_1$ **ensure positivity**

Total 3 parameters

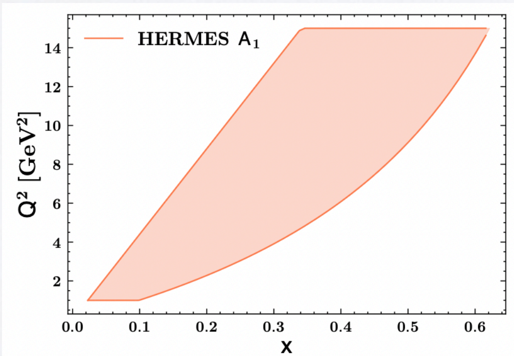

same kin. cuts as MAPTMD22: only Hermes A_1 data survive, exclude CLAS6 & Compass

N = 291 pts. **χ^2/N = 1.09**

Airapetian et al. (Hermes), P.R. D**99** (19) 112001

MAPTMD22pol Helicity TMD PDF

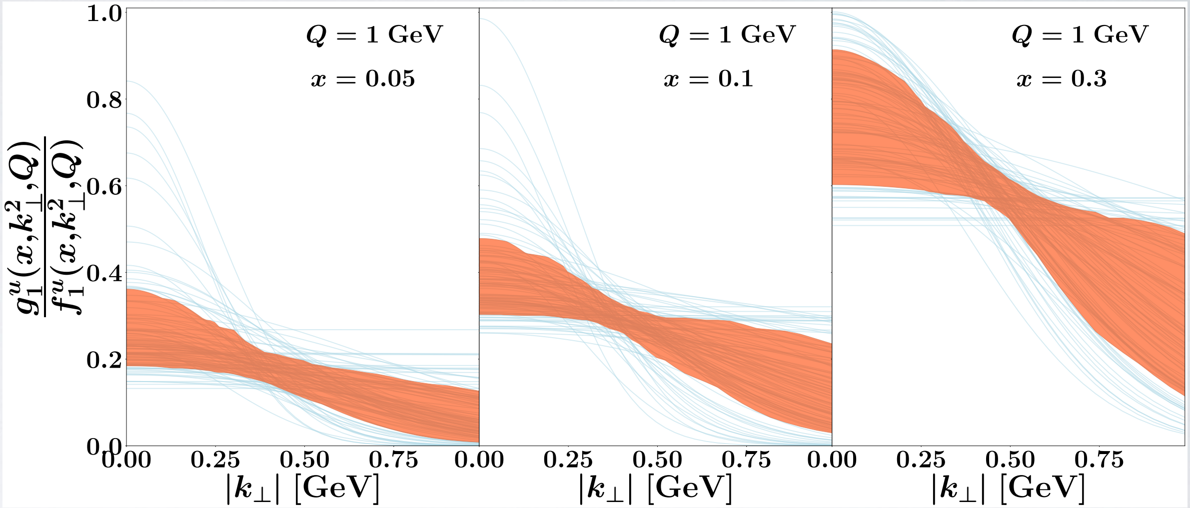

MAPTMD22pol

Bacchetta et al. (MAP),
P.R.L. **134** (25) 121901

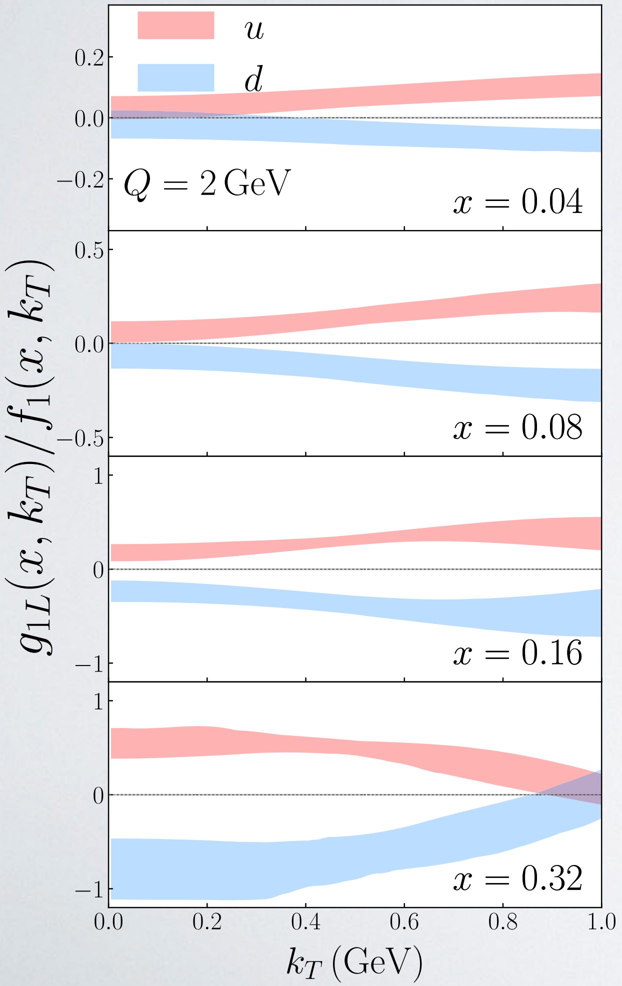

YLSZM

Yang et al.,
P.R.L. **134** (25) 121902

MAPTMD22pol Helicity TMD PDF

input from lattice
$$\frac{g_{1L}^{\Delta u_+ - \Delta d_+}(x, b_T; \mu, \zeta)}{g_A\, f_1^{u_v - d_v}(x, b_T; \mu, \zeta)} \qquad \mu = \sqrt{\zeta} = 1.62 \text{ GeV}$$

(see talk by S.Mukherjee)

Bollweg et al., arXiv:2505.18430

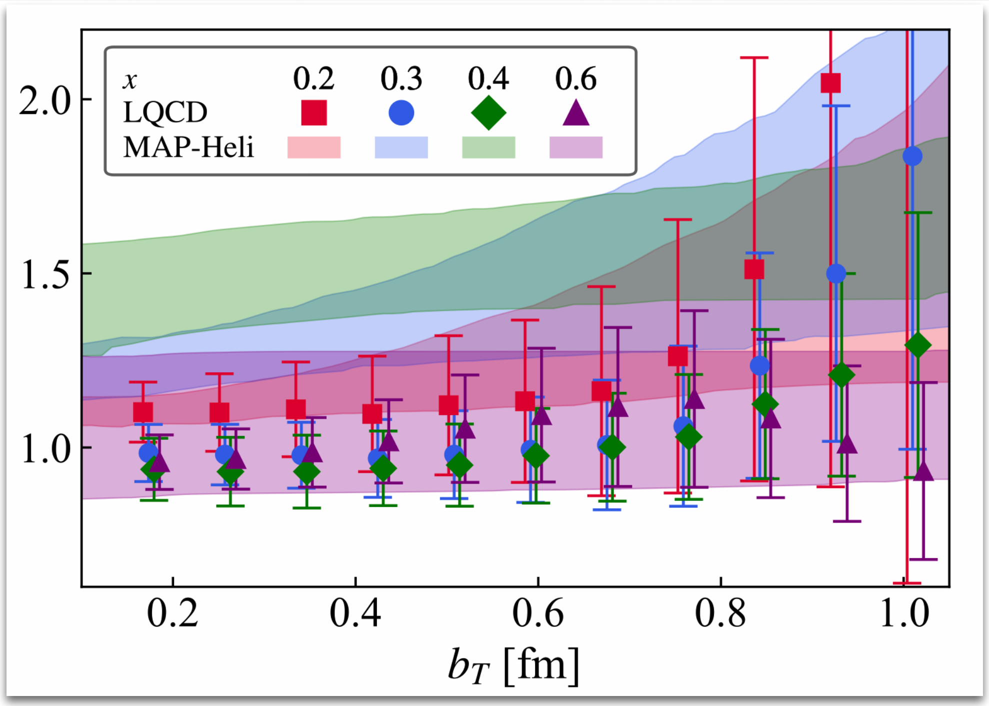

MAPTMD22pol Helicity TMD PDF

input from lattice $\dfrac{g_{1L}^{\Delta u_+ - \Delta d_+}(x, b_T; \mu, \zeta)}{g_A\, f_1^{u_v - d_v}(x, b_T; \mu, \zeta)}$ $\mu = \sqrt{\zeta} = 1.62$ GeV

(see talk by S.Mukherjee)

compatibility for x=**0.2**, **0.6**
partial " for x=**0.3**, **0.4**

Bollweg et al., arXiv:2505.18430

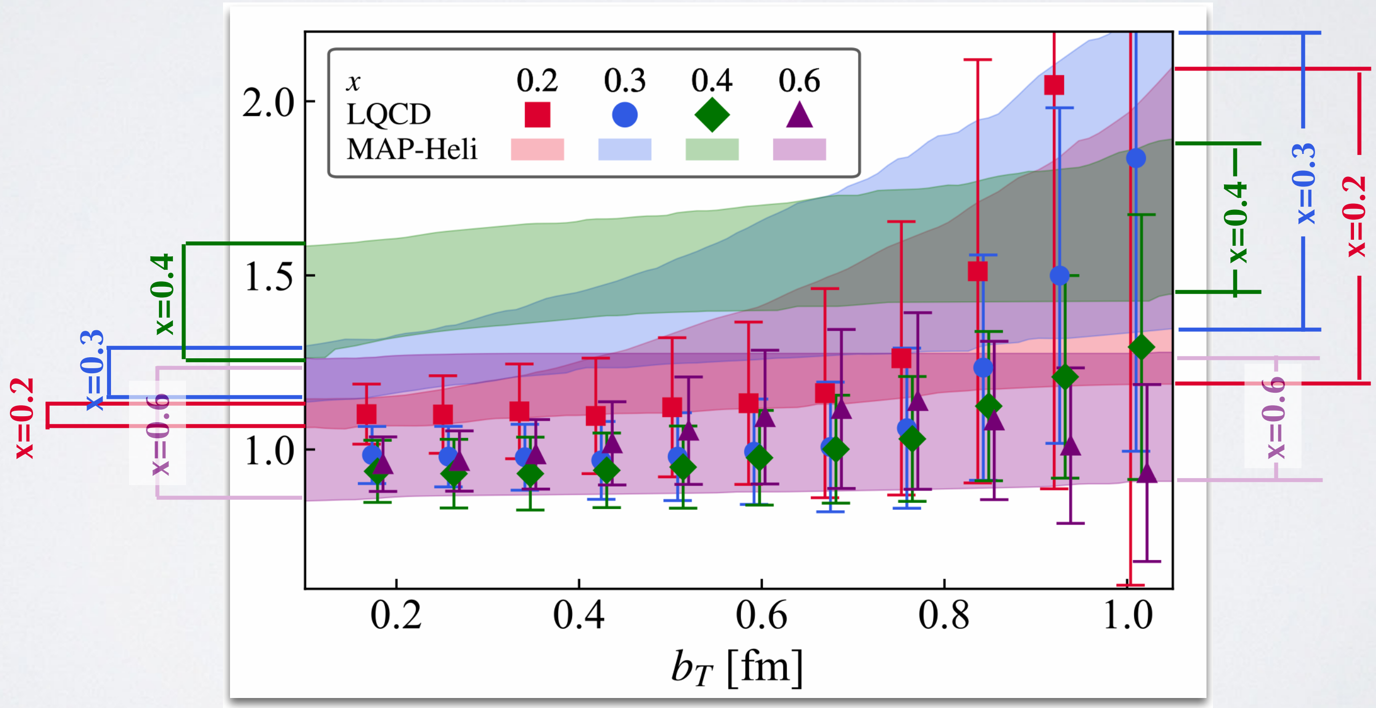

MAPTMD22pol Helicity TMD PDF

input from lattice $\dfrac{g_{1L}^{\Delta u_+ - \Delta d_+}(x, b_T; \mu, \zeta)}{g_A\, f_1^{u_v - d_v}(x, b_T; \mu, \zeta)}$ $\mu = \sqrt{\zeta} = 1.62$ GeV

(see talk by S.Mukherjee)

Bollweg et al., arXiv:2505.18430

compatibility for x=**0.2**, **0.6**
partial " for x=**0.3**, **0.4**

?

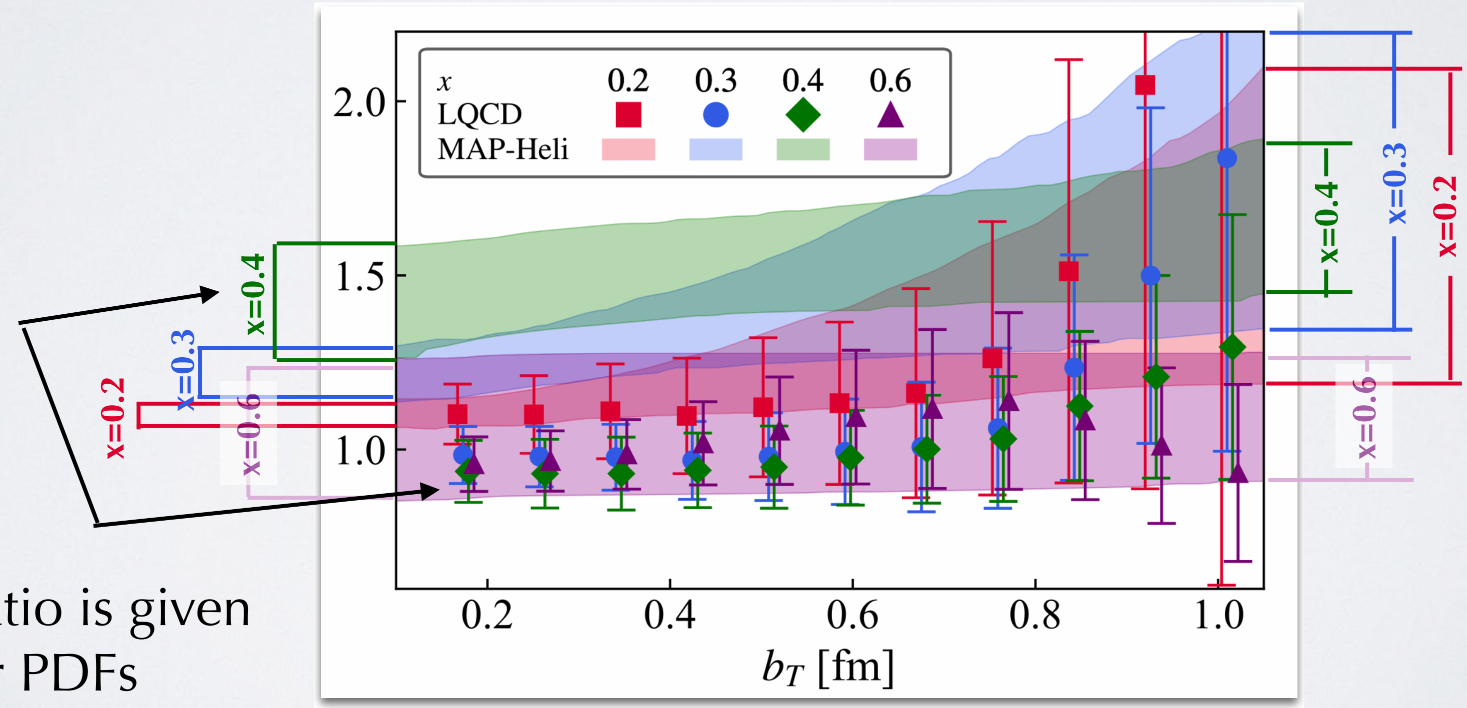

at b_T = 0, ratio is given by collinear PDFs

The Sivers TMD PDF

polarizations quark nucleon

Nucleon Polarization	Quark polarization: Unpolarized (U)	Longitudinally Polarized (L)	Transversely Polarized (T)
U	$f_1 =$		$h_1^\perp =$ -
L		$g_1 =$ -	$h_{1L}^\perp =$ -
T	$f_{1T}^\perp =$ -	$g_{1T} =$ -	$h_1 =$ - $h_{1T}^\perp =$ -

Bacchetta et al., P.L. ***B827*** *(22) 136961, arXiv:2004.14278*

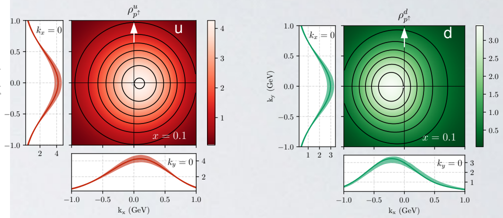

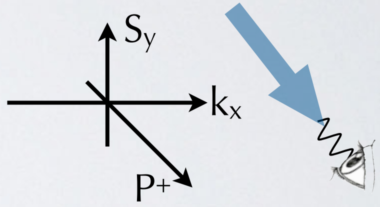

$$\frac{1}{2}\mathrm{Tr}[\Phi\,\gamma_+] \to f_1 - f_{1T}^\perp \frac{(\mathbf{k}_\perp \times \mathbf{S}_T)\cdot\hat{\mathbf{P}}}{M}$$

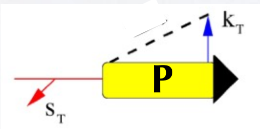

$$\mathbf{S}_T \cdot \mathbf{k}_\perp \times \mathbf{P}$$

Sivers effect: how the momentum distribution of quarks is distorted by the transverse polarization of parent nucleon ("spin-orbit" correlation)

Sivers $f_{1T}^\perp \to$ indirect access to quark orbital angular momentum

Burkardt, P.R. D66 (2002) 114005; N.P. **A735** (2004) 185
Bacchetta & Radici, P.R.L. **107** (2011) 212001
Ji et al., N.P. **B652** (2003) 383

Most recent Sivers extractions

	Framework	SIDIS	DY	W/Z production	forward EM jet	N. of points	χ^2/N	
JAM 2020 arXiv:2002.08384	generalized parton model	✔	✔	✔	✘	517	1.04	
PV 2020 arXiv:2004.14278	LO+NLL	✔	✔	✔	✘	125	1.08	
EKT 2020 arXiv:2009.10710	NLO+N²LL	✔	✔	✔	✘	226/452	0.99 /1.45	SIDIS / +STAR
BPV 2020 arXiv:2012.05135 arXiv:2103.03270	ζ prescription	✔	✔	✔	✘	76	0.88	
TO-CA 2021 arXiv:2101.03955	generalized parton model	✔	✘	✘	✔	238	$1.05^{+0.03}_{-0.01}$	SIDIS + reweighting
JAM 2022 arXiv:2205.00999	generalized parton model	✔	✔	✔	✘	255	1.10	+ A_N^π data
Fernando-Keller arXiv:2304.14328	generalized parton model	✔	✔	✘	✘	732	1.66	

lower accuracy and less data w.r.t. unpolarized TMD

Most recent Sivers extractions

	Framework	SIDIS	DY	W/Z production	forward EM jet	N. of points	χ^2/N	
JAM 2020 arXiv:2002.08384	generalized parton model	✔	✔	✔	✘	517	1.04	
PV 2020 arXiv:2004.14278	LO+NLL	✔	✔	✔	✘	125	1.08	
EKT 2020 arXiv:2009.10710	NLO+N^{2}LL	✔	✔	✔	✘	226/452	0.99 /1.45	SIDIS / +STAR
BPV 2020 arXiv:2012.05135 arXiv:2103.03270	ζ prescription	✔	✔	✔	✘	76	0.88	
TO-CA 2021 arXiv:2101.03955	generalized parton model	✔	✘	✘	✔	238	$1.05^{+0.03}_{-0.01}$	SIDIS + reweighting
JAM 2022 arXiv:2205.00999	generalized parton model	✔	✔	✔	✘	255	1.10	+ A_N^π data
Fernando-Keller arXiv:2304.14328	generalized parton model	✔	✔	✘	✘	732	1.66	

first using Neural Networks, but limited analysis:

- parton model => no TMD evolution
- no consistent knowledge of unpolarized TMD in denominator of spin asymmetry

Most recent Sivers extractions

first k_T-moment $f_{1T}^{\perp(1)}(x)$

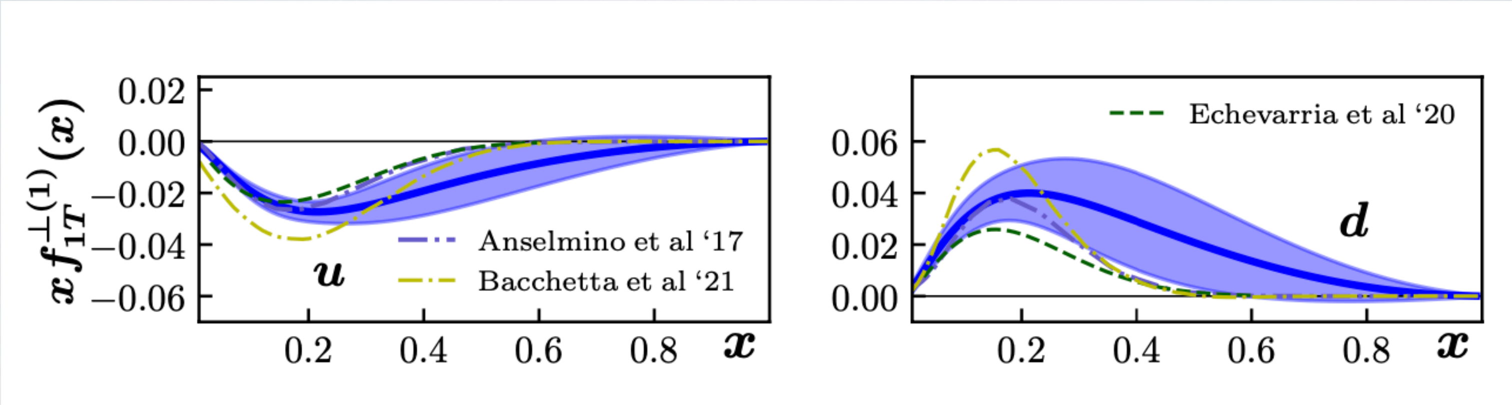

all parametrizations are in fair agreement for x-dependence of valence flavors

k_T-dependence is still much unconstrained

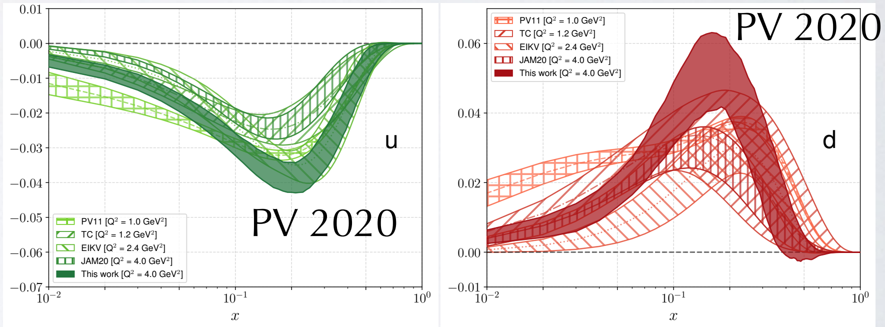

Bacchetta et al., P.L. ***B827*** *(22) 136961 arXiv:2004.14278*

sea-quarks ~ $O(10^{-3})$ smaller, large errors

=> impact of EIC

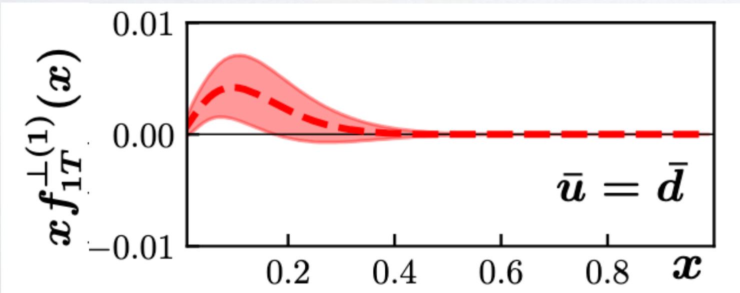

Sign change puzzle

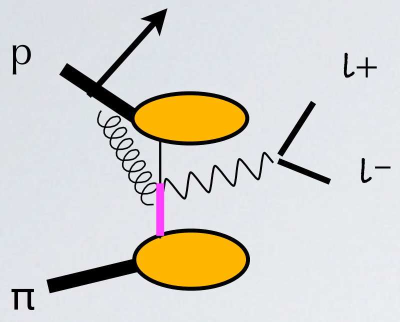

π-p↑ Drell-Yan

spin asymmetry

$A_T \sim f_{1,\pi} \otimes f_{1T,p}^{\perp}$

Aghasyan et al., P.R.L. ***119*** *(17) 112002*

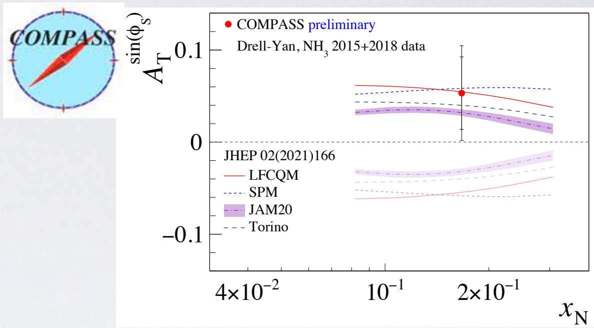

sign change

no sign change

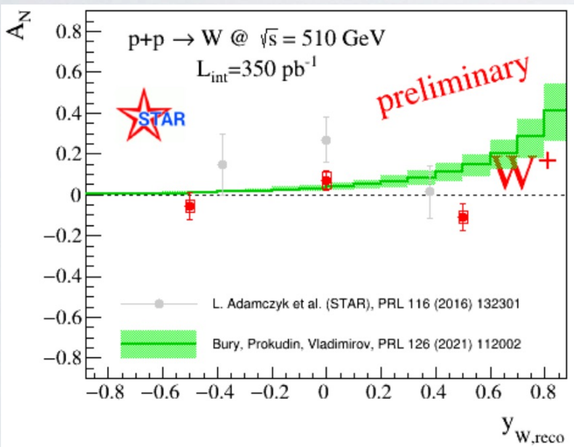

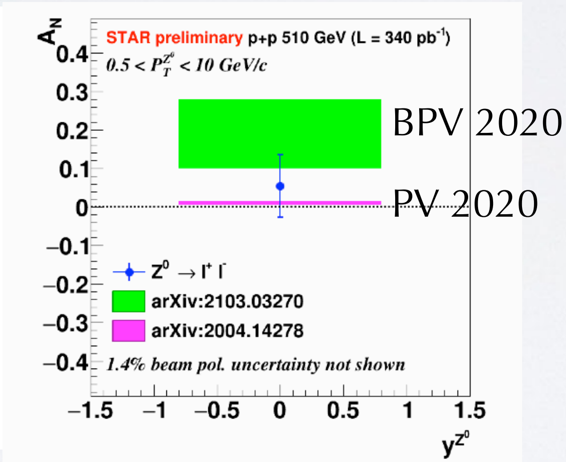

p-p↑ → W+X
p-p↑ → Z⁰+X

$A_N \sim f_{1,p} \otimes f_{1T,p}^{\perp}$

Adamczyk et al., P.R.L. ***116*** *(16) 132301*

still not enough to confirm sign change

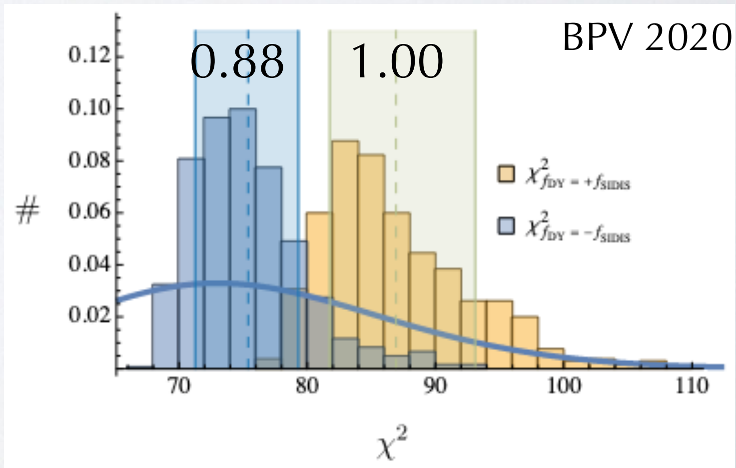

Transversity

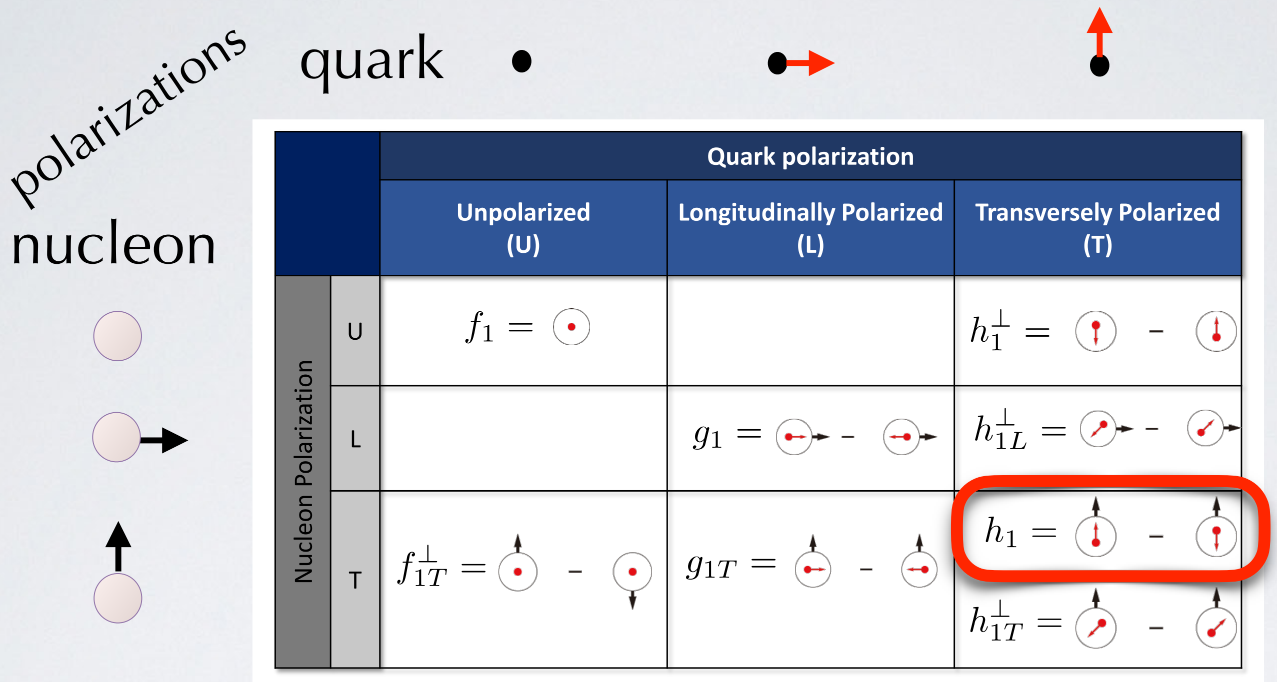

- transversity is the prototype of chiral-odd structures
- the only chiral-odd structure that survives in collinear kinematics
- only way to determine the tensor charge $\delta^q(Q^2) = \int_0^1 dx\, h_1^{q-\bar{q}}(x, Q^2)$

Most recent extractions

Collins effect	Framework	e+e-	SIDIS	Drell-Yan A_N	Lattice
Anselmino 2015 P.R. **D92** (15) 114023	parton model	✔	✔	✘	✘
Kang et al. 2016 P.R. **D93** (16) 014009	TMD / CSS	✔	✔	✘	✘
Lin et al. 2018 P.R.L. **120** (18) 152502	parton model	✘	✔	✘	✔ g_T
D'Alesio et al. 2020 (CA) P.L. **B803** (20) 135347	parton model	✔	✔	✘	✘
JAM3D-20 P.R. **D102** (20) 054002	parton model	✔	✔	✔	✘
JAM3D-22 P.R. **D106** (22) 034014	parton model	✔	✔	✔	✔ g_T
Boglione et al. 2024 (TO) P.L. **B854** (24) 138712	parton model	✔	✔	✔ reweighting	✘

Dihadron mechanism	e+e- unpol. $d\sigma^0$	e+e- asymmetry	SIDIS	p-p collisions	Lattice
Radici & Bacchetta 2018 P.R.L. **120** (18) 192001	PYTHIA (separately)	✔ (separately)	✔	✔	✘
Benel et al. 2020 E.P.J. **C80** (20) 5	PYTHIA (separately)	✔ (separately)	✔	✘	✘
JAMDIFF 2024 P.R.L. **132** (24) 091901	✔	✔	✔	✔	✔ δu, δd

Transversity

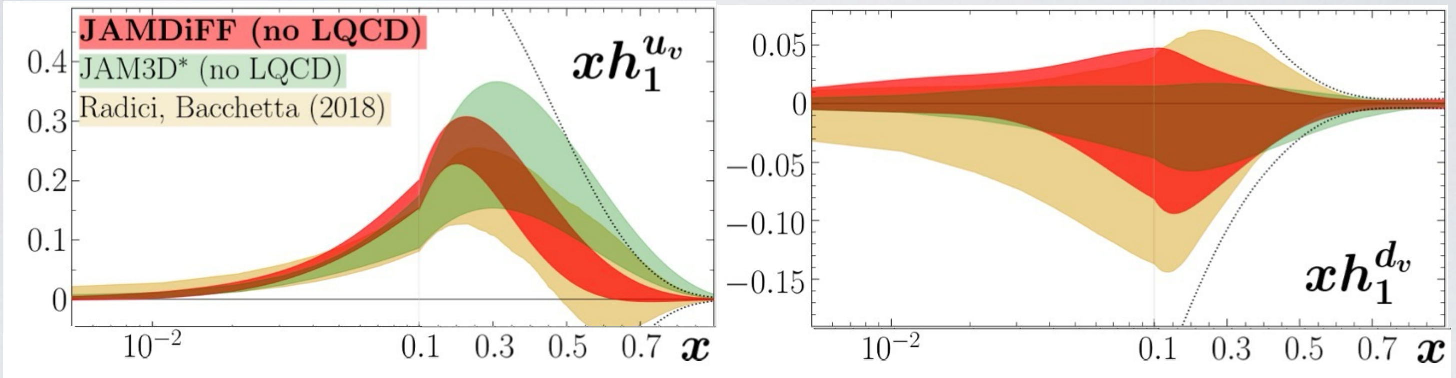

D. Pitonyak, QCD Evolution 24

* JAM3D includes $\bar{u} = -\bar{d}$ w.r.t. JAM22

consistency of phenomenological extractions from a variety of exp. data with different approaches
(provided that no LQCD points are included in the fit)

Pheno - lattice : tensor charge

$g_T = \delta u - \delta d$

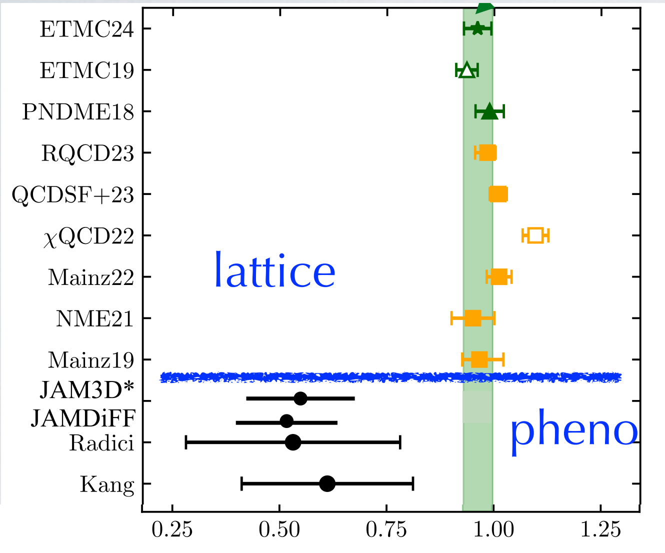

adapted from C. Alexandrou, QCD Evolution 24

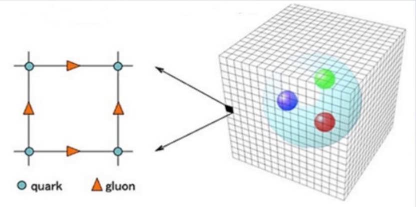

green N_f=2+1+1

open symbols = no continuum extrapolation

yellow N_f=2+1

tension between pheno and lattice ?

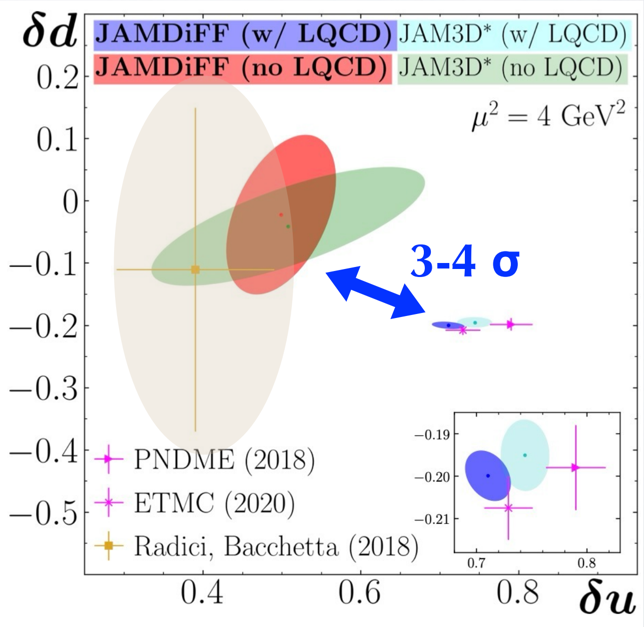

adapted from D. Pitonyak, QCD Evolution 24

Pheno - lattice : tensor charge

$g_T = \delta u - \delta d$

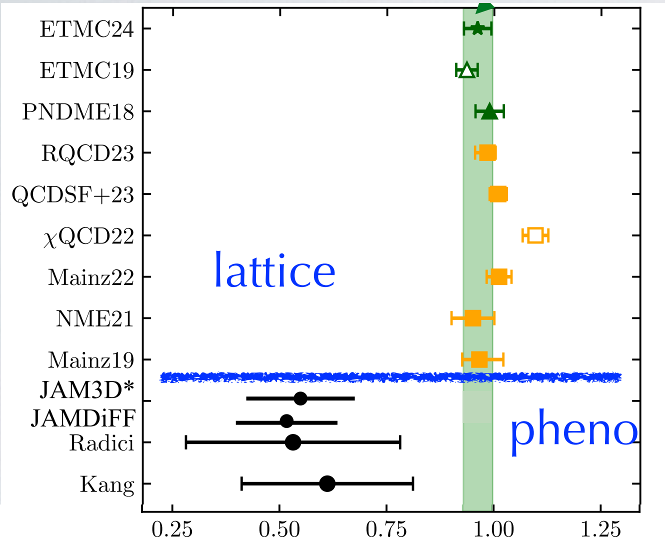

adapted from C. Alexandrou, QCD Evolution 24

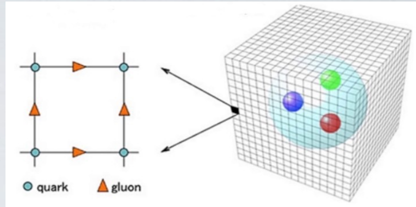

green N_f=2+1+1

open symbols = no continuum extrapolation

yellow N_f=2+1

tension between pheno and lattice ?

Including lattice data,
JAM finds **compatibility,**
still under discussion…

Experiment	N_{dat}	χ^2_{red} With LQCD	χ^2_{red} No LQCD
Belle (cross section) [63]	1094	1.01	1.01
Belle (Artru-Collins) [92]	183	0.74	0.73
HERMES [94]	12	1.13	1.10
COMPASS (p) [95]	26	1.24	0.75
COMPASS (D) [95]	26	0.78	0.76
STAR (2015) [96]	24	1.47	1.67
STAR (2018) [64]	106	1.20	1.04
ETMC δu [28]	1	0.71	…
ETMC δd [28]	1	1.02	…
PNDME δu [25]	1	8.68	…
PNDME δd [25]	1	0.04	
Total χ^2_{red} (N_{dat})		1.01 (1475)	0.98 (1471)

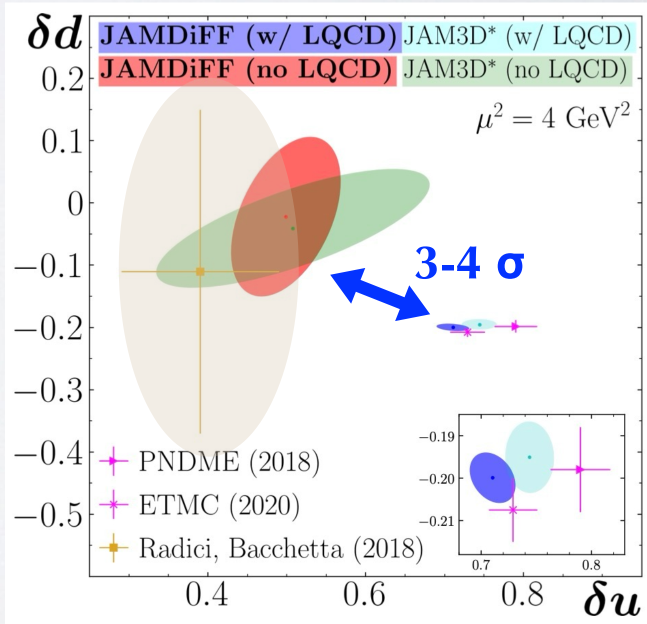

adapted from D. Pitonyak, QCD Evolution 24

Pheno - lattice : tensor charge

$g_T = \delta u - \delta d$

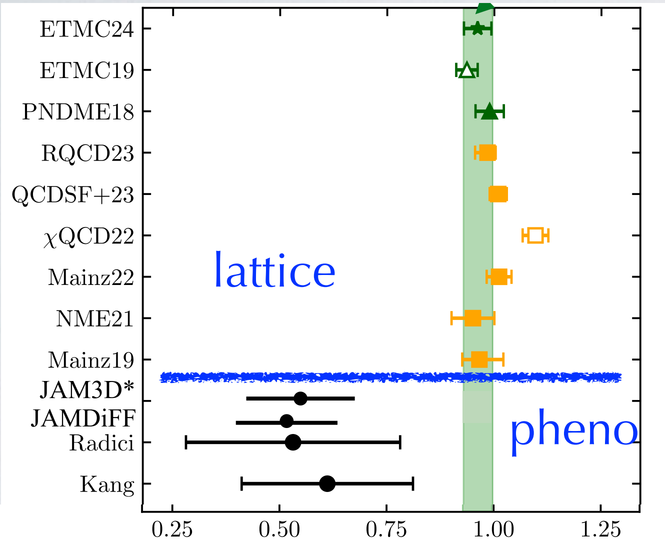

adapted from C. Alexandrou, QCD Evolution 24

green N_f=2+1+1

open symbols = no continuum extrapolation

yellow N_f=2+1

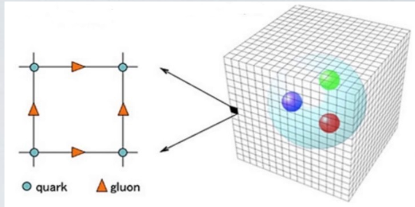

tension between pheno and lattice ?

Including lattice data, JAM finds **compatibility,** **still under discussion…**

But most data insensitive to tensor charge

?

Experiment	N_{dat}	χ^2_{red} With LQCD	χ^2_{red} No LQCD
Belle (cross section) [63]	1094	1.01	1.01
Belle (Artru-Collins) [92]	183	0.74	0.73
HERMES [94]	12	1.13	1.10
COMPASS (p) [95]	26	1.24	0.75
COMPASS (D) [95]	26	0.78	0.76
STAR (2015) [96]	24	1.47	1.67
STAR (2018) [64]	106	1.20	1.04
ETMC δu [28]	1	0.71	…
ETMC δd [28]	1	1.02	…
PNDME δu [25]	1	8.68	…
PNDME δd [25]	1	0.04	…
Total χ^2_{red} (N_{dat})		1.01 (1475)	0.98 (1471)

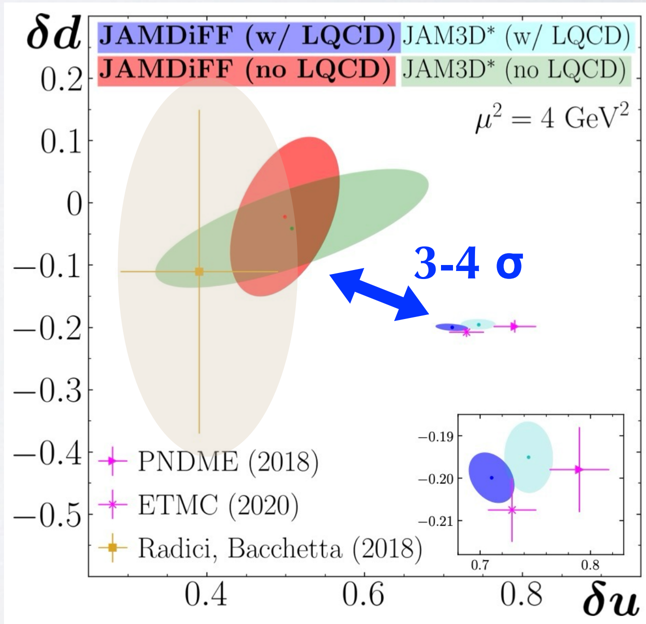

adapted from D. Pitonyak, QCD Evolution 24

List of latest extractions

Nucleon Polarization	Quark polarization: Unpolarized (U)	Longitudinally Polarized (L)	Transversely Polarized (T)	
U	$f_1 =$		$h_1^\perp =$	Boer-Mulders
L		$g_1 =$	$h_{1L}^\perp =$	Kotzinian-Mulders
T	$f_{1T}^\perp =$	$g_{1T} =$	$h_1 =$ $h_{1T}^\perp =$	pretzelosity

worm gear

(Kotzinian-Mulders)

Boer-Mulders	arXiv:2004.02117, arXiv:2407.06277
Worm-gear g1T	arXiv:2110.10253, arXiv:2210.07268
Worm-gear h1L	
Pretzelosity	arXiv:1411.0580

courtesy A. Bacchetta

not mentioned pion TMDs, TMD fragmentation functions, nuclear TMDs

Summary

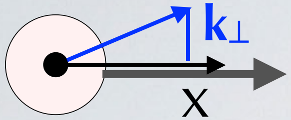

TMD PDFs (x, $k_\perp$; Q^2) at leading twist for a spin-1/2 hadron (Nucleon)

quark

nucleon

Nucleon Polarization	Quark polarization: Unpolarized (U)	Quark polarization: Longitudinally Polarized (L)	Quark polarization: Transversely Polarized (T)	nomenclature
U	$f_1 =$		$h_1^\perp =$ −	unpolarized; Boer-Mulders
L		$g_1 =$ −	$h_{1L}^\perp =$ −	helicity; Kotzinian-Mulders
T	$f_{1T}^\perp =$ −	$g_{1T} =$ −	$h_1 =$ − $h_{1T}^\perp =$ −	transversity; pretzelocity
	Sivers	worm gear		

- very good knowledge of x-dependence of f_1 and g_1
- good knowledge of k_T-dependence of f_1
- fair knowledge of x-dependence of h_1 and k_T-moments of $f_{1T}^\perp$
- some hints about all others

for discussion

- what is the meaning of $f_1(x, b_T=0) = 0$?

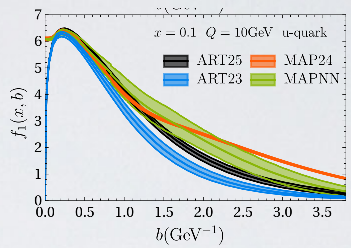

shouldn't we look at TMDs in k_T space ??

- is positivity ensured if $D_1(z, b_T) < 0$?

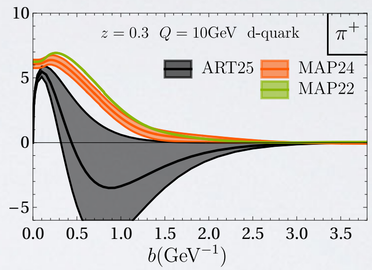

- ratios $f_1(u)/f_1(d)$ and g_1/f_1 at $b_T=0$ should reproduce the ratio of corresponding collinear PDFs…

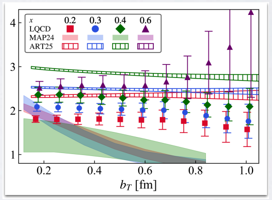
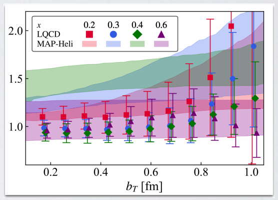

- what are the limits of TMD factorization ?

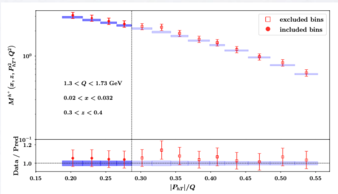

$$q_T^2 = \frac{P_{hT}^2}{z^2} \ll Q^2 \quad ?$$

- has the tension between phenomenology and lattice tensor charge been really solved ?